Stony Brook University

Interactive Dimensional Synthesis of Spherical 6R Closed Chains and Planar Parallel Manipulators via Constraint Manifold Modification

A Thesis Presented
by

Aditya Gupta

to

The Graduate School
in partial fulfillment of the
Requirements
for the degree of

Master of Science
in
Mechanical Engineering

Stony Brook University
May 2010

Stony Brook University
The Graduate School
Aditya Gupta
We, the thesis committee for the above candidate for the
Master of Science degree,
hereby recommend acceptance of this thesis.

Dr. Anurag Purwar, Advisor,
Research Assistant Professor, Mechanical Engineering Department

Dr. Q. Jeffrey Ge,Co-Advisor
Professor, Mechanical Engineering Department

Dr. Yu Zhou, Chairman of Thesis Committee,
Assistant Professor, Mechanical Engineering Department

This thesis is accepted by the Graduate School.

Lawrence Martin
Dean of the Graduate School

Abstract of the Thesis

Interactive Dimensional Synthesis of Spherical 6R Closed Chains and Planar Parallel Manipulators via Constraint Manifold Modification

by

Aditya Gupta

Master of Science

in

Mechanical Engineering

Stony Brook University

2010

In this thesis the dimensional synthesis of a spherical 6R closed chain and a class of planar parallel manipulator is discussed.

The kinematic constraints of the planar as well as the spherical mechanisms relate to the constraints that limit the position of the links of planar and spherical closed chains in the Cartesian space. Quaternions are used to represent planar and spherical displacements. The problem of synthesizing smooth piecewise rational motions is converted into that of designing smooth piecewise rational curves in the space of quaternions(image space). The kinematic constraints are transformed into geometric constraints for the design of quaternion image curves.

An interactive, user friendly graphical tool is used for dimensional synthesis. The graphical tool allows the user to visually contain the image curve by simple geometric manipulation of the size, orientation, and the location of

the constraint surfaces that is developed. The process is intuitive and lends designers an understanding of the mechanism design methodology.

Table of Contents

List of Figures

List of Tables

ACKNOWLEDGEMENTS

I take this opportunity to thank my research advisor, Prof. Anurag Purwar, for his guidance and invaluable support throughout my academic and research term at Stony Brook University. He has extensive knowledge of subject, which he willing shared with me. It is because of him I have successfully been able to complete my thesis.

I would also like to extend my thanks to Prof. Yu Zhou for agreeing to chair my thesis committee and Prof. Jeff Ge for helping me as my co-advisor. In addition I would like to thank all the committee members for their time and valuable suggestions. Jun Wu has helped me with his suggestions and I would like to thank him for his friendship.

My parents and my sister have been my backbone and have stood by me throughout. I am indebted to them, all this would not have been possible without their encouragement and faith in my capabilities. Last but not the least, my close friends at Stony Brook University made experience a memorable one, I cannot thank them enough.

As a graduate student of Stony Brook University, I have learned at lot and grown as a person, in the past two years. The environment here has been educating, inspiring and pleasant. I am now confident and well rounded in all specialties and have a vision of how I see myself grow in the future, I owe a lot to Prof. Anurag Purwar, my advisor and mentor.

Chapter 1

Introduction and Background

This thesis deals with the dimensional synthesis of spherical 6R and planar parallel manipulators. This chapter gives a general overview of the existing work in the area of dimensional synthesis of 6R closed chain and planar parallel manipulator.

Mechanisms are usually designed for three kinds of purposes: 1. function generation, 2. path generation or 3. motion generation. We are concerned with the dimensional synthesis of spherical 6R mechanisms and planar parallel manipulators for motion generation, that is, to guide a rigid body through a given rational motion. Rational motions are defined by a ratio of two polynomial functions and are compatible with the industry standard Non-Uniform Rational B-splines (NURBS) based CAD/CAM systems.

The past two decades have witnessed a significant body of work emanating from the application of well-known curve and surface design algorithms from computer aided geometric design(CAGD) to the field of theoretical kinematics for the purpose of developing rational Bezier and B-Spline motions of rigid

bodies. The idea behind such a synergy is that the problem of designing rational curves in a higher dimensional projective space via a special mapping. By choosing the quaternion representation of the displacement and orientation, the problem is further reduced to designing curves in the space of quaternions. Rational motions, with applications spanning across areas such as motion animation in computer graphics, task specification in mechanism synthesis, and virtual reality systems as well as Cartesian motion planning in robotics, are an attractive proposition since they integrate well the industry standard nonuniform rational B-spline(NURBS) based computer aided design/computer aided manufacturing(CAD/CAM) system. Furthermore, from a computational perspective they can easily exploit fast and stable algorithms from CAGD.

Theory of mechanisms synthesis is well-developed (see Sandor and Erdman [1], Suh and Radcliffe [2], and McCarthy [3]), and there has been a great deal of academic research in the development of software systems for the synthesis of mechanisms (KINSYN III from Rubel and Kaufamn [4], LINCAGES from Erdman and colleagues [5, 6], Kihonge et al. [7], Spades from Larochelle [8], Perez and McCarthy [9], Su and McCarthy [10], Synthetica from Su et al. [11]). In the commercial domain, SyMech [12] and WATT [13] are two well-known software systems for planar mechanisms design. For computer aided design of spherical mechanisms, McCarthy, Larochelle, Vance, and colleagues have devoted their efforts to the design of spherical 4R mechanisms in traditional Human Computer Interaction (HCI) as well as virtual reality (VR) environment for the motion guidance through a given number of positions (see Sphinx

from Larochelle et al. [14], Sphinxpc from Ruth and McCarthy [15], SphinxVR from Furlong et al. [16], Osiris from Tse and Larochelle [17]). Ketchel and Larochelle [18] also developed SphinxCAM to aid in automated assembly and manufacturing of spherical 4R mechanisms designed in systems such as Sphinx and Osiris. Kraal and Vance et al. [19] recognized the need to develop user interfaces that were better suited to the cognitive and perceptive nature of designers. Their efforts led to VEMCES, a virtual reality interface for spherical 4R mechanism design.

Spherical mechanisms constrain the motion of a moving object on the surface of a sphere and all the moving surfaces are concentric spheres. They are known to be compact and provide a wide range of transmission characteristics (Chiang [20]).

A parallel manipulator consists of a moving platform that is connected to the base by several legs. Another definition is given by (Merlet 2006 [21]): a generalized parallel manipulator is a closed-loop kinematic chain mechanism whose end-effector is linked to the base by several independent kinematic chains.

The general approach of the work presented is closely related to the kinematic mapping approach for dimensional synthesis of planar and spherical mechanisms pioneered by Ravani and Roth [22]. Their work was followed by Bodduluri and McCarthy [23], Bodduluri [24], and Larochelle [25]. Their approach involved minimizing the distance error between the given positions and the image curve of the chain. This resulted in approximate motion synthesis.

Brunnthaler et.al. [26] used kinematic mapping to solve the problem of designing a spherical four-bar mechanism that interpolates a coupler through five given orientations. Venkataramanujam and Larochelle [27] and Larochelle [28] used parameterized constraint manifold and employed nonlinear optimization to give numerical methods for approximate motion synthesis of open and closed chains.

To study the dimensional synthesis problem from the perspective of constrained motion interpolation. Jin and Ge [29, 30] and Purwar et al. [31, 32, 33] have studied the problem of motion interpolation under kinematic constraints for planar and spherical 2R, 3R open, and 6R closed chains as well as spatial SS chains. By using quaternions or dual quaternions and kinematic mapping approach they transformed the problem of constrained motion interpolation into designing a rational curve constrained to satisfy geometry of the constraint manifold. Starting with an initial unconstrained curve, they modify the curve using an iterative numerical method until it fits inside the constraint manifold. The current work investigates the inverse problem, that is, to change the constraint manifold while keeping the given rational curve fixed for dimensional synthesis of spherical 6R and planar parallel mechanisms. Jun et al. [34] designed and developed a system for the dimensional synthesis of planar 6R mechanisms; this work is an extension of that to the spherical mechanisms as well as to the planar parallel manipulators.

The design method treats a spherical 6R closed chain as a mechanism assembled together using two open chains connected at the ends. Whereas a

planar parallel manipulator is treated as three open chains connected to a moving platform. Each open chain imposes kinematic constraints that limit the positions and orientations of the object connected to the end link. We use the algebraic form of the constraint manifold (McCarthy [35] and Ge [36]) for the spherical 6R closed chains and Jin [37] for the planar open chains. Thus, the kinematic constraints are transformed into geometric constraints, and the given rational motion is transformed into a rational curve in the image space. This way, the problem reduces to finding the constraint manifold that accommodates the given rational curve. Algebraically, the kinematic constraints are derived in the inequality form, where the limits of the inequalities are functions of link lengths, while the constraint functions themselves incorporate parameters that describe the location and orientation of fixed and moving frames. In the end, we design open chains that simultaneously satisfy the kinematic constraints and the motion requirements. A visual interpretation of this approach is that we find the smallest possible constraint manifold that will contain the given image curve entirely.

The parallel manipulators have very advantageous as compared to serial manipulators. As they possess excellent load to weight ratio, high stiffness and positioning accuracy and good dynamic behavior.(Merlet 2006 [21]) In contrast to a serial manipulator the load is often carried as a cantilever. The positioning error of the end effector tend to average out in a parallel manipulator whereas its cumulative in serial manipulators. All of these advantages have increased the use of parallel manipulators as compared to serial manipulators.

In industry and scientific facilities, parallel manipulators are widely used for different areas such as flight simulations, high speed and high precision machining center, pointing devices, medical applications, mining machines, walking machines, adjustable articulated trusses and etc.

Figure 1.1: A parallel manipulator being used in manufacturing process. Source: courtesy of Mikrolar Inc.(http://mikrolar.com/industrial.html)

Figure 1.2: 5 Axis Water-Jet Cutting System. Source: courtesy of Mikrolar Inc.(http://mikrolar.com/waterjet.html)

The rest of the thesis is organized as follows. Chapter 2 deals with kinematic constraint of planar parallel manipulator. Chapter 3 deals with kinematic constraint of spherical 3R open chain and spherical 6R closed chain. Chapter 4 is a guide to use the software tool developed for dimensional synthesis. The final chapter summarizes the work of this research and makes a few salient points regarding the future development of this work.

Chapter 2

Kinematic Constraints of Planar Parallel Manipulator

2.1 Introduction

This chapter deals with the formulation of kinematic constraints of planar parallel manipulator using quaternion based representation found in McCarthy [35] and Ge [36].

The organization of this chapter is as follows. Section 2.2 explains the classification of planar parallel manipulators, Section 2.3 explains planar displacements and planar quaternions and Section 2.4 presents the constraint manifolds of different types of planar open chain

2.2 Classifying General Planar Three-Legged Parallel Manipulators

A three legged parallel manipulator is a closed-loop kinematic chain whose end-effectors are linked to a base (platform) by three independent kinematic

chains. Each chain is connected by three independent one DOF joints, one of which is active. Since the displacements of the platform is confined to the plane, only Rotary(R) and Prismatic(P) pairs are used (Hayes [38]).

The possible combinations of R and P in a three-legged platform are:

RRR,RPR,RRP,RPP,PRR,PPR,PRP,PPP

The PPP chain must be excluded because this combination will give rise to translations only with no change in orientation. Thus, there are seven possible kinematic chains.

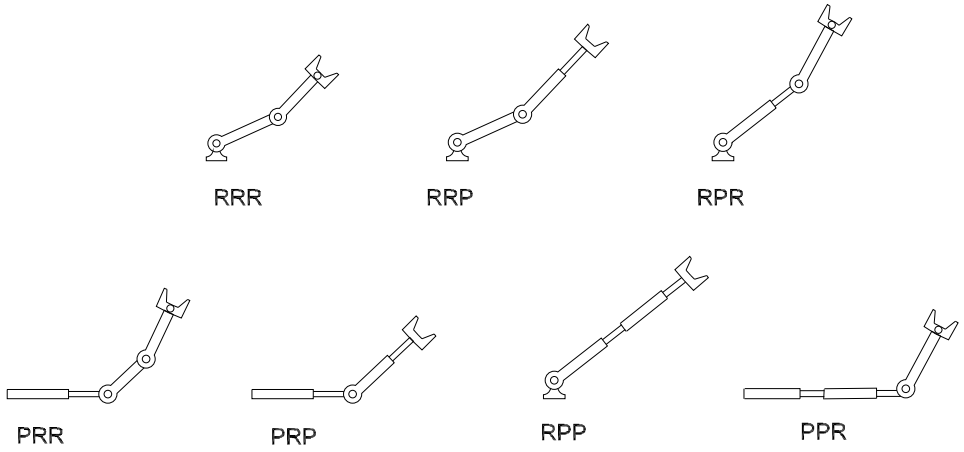

Figure 2.1: The seven possible leg topologies

The active joint in a leg is identified with an underscore, R$\underline{\text{P}}$R, for example. Since any one of the three joints in any of the seven allowable simple kinematic chains may be actuated there are twenty-one possible leg architectures. When the value of the actuated joint input in a leg is specified, the joint is effectively

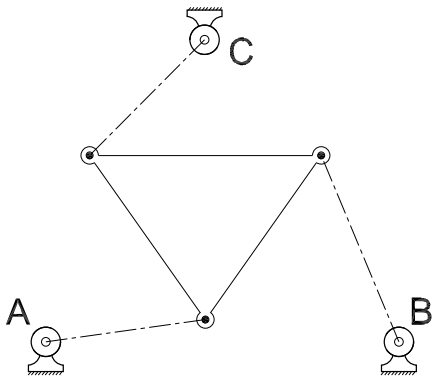

Figure 2.2: Three legged planar parallel manipulator

locked and may be conceptually removed, temporarily, from the chain. What remains is a kinematic chain connected with two passive joints. It is seen that the resulting passive sub-chain is one of only four types: either RR, PR, RP, or PP. For the moment we exclude PP-type legs from the enumeration since platforms containing two or three such legs either move uncontrollably or are not assemblable when the actuated joint variables are specified Merlet [39] and Hayes [40] . PP type legs are considered separately. This reduces the number of possible leg architectures presently under consideration from twenty-one to eighteen. They are listed, according to passive sub-chain, in table below:

The platform is considered to be symmetric when all three legs are the same type, each possessing the same type of actuated joint at the same location in the kinematic chain. The leg is otherwise considered to be asymmetric.

RR-type	PR-type	RP-type
$\underline{\text{R}}$RR	$\underline{\text{R}}$PR	$\underline{\text{R}}$RP
R$\underline{\text{R}}$R	P$\underline{\text{R}}$R	R$\underline{\text{R}}$P
RR$\underline{\text{R}}$	PR$\underline{\text{R}}$	RP$\underline{\text{R}}$
$\underline{\text{P}}$RR	$\underline{\text{P}}$PR	$\underline{\text{P}}$RP
R$\underline{\text{P}}$R	P$\underline{\text{P}}$R	R$\underline{\text{P}}$P
RR$\underline{\text{P}}$	PR$\underline{\text{P}}$	RP$\underline{\text{P}}$

Table 2.1: 18 of 21 possible lower pair leg architectures

This number is arrived at by first considering the 18 kinematic chains in Table 1 to choose from for each leg. A selection of r different elements taken from a set of n, without regard to order, is a combination of the n elements taken r at a time. If the elements are allowed to be counted more than once the number of possible combinations is given by

$$C(n,r) = \frac{n!}{r!(n-r)!} \tag{2.1}$$

$$\text{C(18,3)} = 816$$

There are, in addition, three possible PP-type legs: RPP, PRP, and PPR. However, a platform can only contain one PP-type leg. This one leg can be combined with any of the 18 listed in Table 1. The total number of platforms containing a single PP-type leg can therefore be counted as:

$$3(\text{C(18,2)}) = 459$$

Combining the results we get the number of all possible general planar three-legged platforms jointed with lower pairs possessing three DOF: 1275

2.3 Planar Displacements and Planar Quaternions

A planar displacement can be represented by a planar quaternion (see Bottema and Roth [41] and McCarthy [35]). Planar quaternions have been used for designing planar open and closed chains (Ravani and Roth [42], Larochelle [43], Murray et al. [44], Perez and McCarthy [45]).

For a planar displacement shown in Figure 2.3, let d_1, d_2 denote the coordinates of the origin of the moving frame $\mathbf{M}$ in the fixed frame $\mathbf{F}$ and α denote the rotation angle of $\mathbf{M}$ relative to $\mathbf{F}$. Then a planar displacement can be represented by a planar quaternion, $\mathbf{Z} = Z_1\epsilon\mathbf{i} + Z_2\epsilon\mathbf{j} + Z_3\mathbf{k} + Z_4$, where $(\mathbf{i}, \mathbf{j}, \mathbf{k}, 1)$ form the quaternion basis and ϵ is the dual unit with the property $\epsilon^2 = 0$. The components of the planar quaternion, $\mathbf{Z} = (Z_1, Z_2, Z_3, Z_4)$, are given by

$$\begin{aligned} Z_1 &= (d_1/2)\cos(\alpha/2) + (d_2/2)\sin(\alpha/2), \\ Z_2 &= -(d_1/2)\sin(\alpha/2) + (d_2/2)\cos(\alpha/2), \\ Z_3 &= \sin(\alpha/2), \\ Z_4 &= \cos(\alpha/2). \end{aligned} \tag{2.2}$$

These four components can be identified as coordinates of a point in four dimensional space. The point $\mathbf{Z}$ is called the *image point of a planar displacement*. The set of image points that represent all planar displacements is called the *image space* of planar displacements and is denoted as Σ_p. In view of (2.2), the coordinates of an image point must satisfy the equation:

$$Z_3^2 + Z_4^2 = 1. \tag{2.3}$$

The above equation may be interpreted as defining a hyper-circular cylinder

in four dimensions.

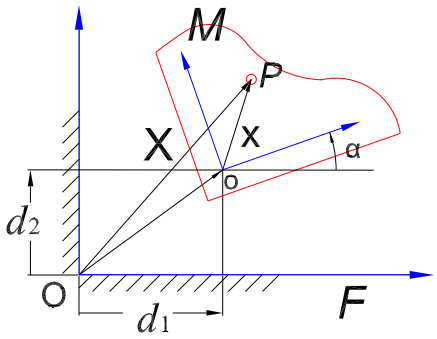

Figure 2.3: A planar displacement.

If the point $\mathbf{x} = (x, y)$ in $\mathbb{R}^2$ is identified with $\mathbf{x} = y\mathbf{i}\epsilon - x\mathbf{i}\epsilon + \mathbf{k}$, then the result of planar displacement of $\mathbf{x}$ is obtained by

$$\mathbf{X} = \mathbf{Z}\mathbf{x}\mathbf{Z}^*, \tag{2.4}$$

where $\mathbf{Z} = Z_4 - Z_1\epsilon\mathbf{i} - Z_2\epsilon\mathbf{j} - Z_3\mathbf{k}$ is the *conjugate* of $\mathbf{Z}$.

We can use homogeneous transform matrix to represent Eq. (2.4):

$$\begin{bmatrix} \mathbf{X} \\ 1 \end{bmatrix} = [A] \begin{bmatrix} \mathbf{x} \\ 1 \end{bmatrix}, \tag{2.5}$$

where

$$[A] = \frac{1}{Z_3^2 + Z_4^2} \begin{bmatrix} Z_4^2 - Z_3^2 & -2Z_3Z_4 & 2(Z_1Z_4 - Z_2Z_3) \\ 2Z_3Z_4 & Z_4^2 - Z_3^2 & 2(Z_1Z_3 + Z_2Z_4) \\ 0 & 0 & Z_3^2 + Z_4^2 \end{bmatrix}. \tag{2.6}$$

Note that when Z_i $(i = 1, 2, 3, 4)$ is replaced by wZ_i, where w is a nonzero scalar, the matrix $[A]$ is unchanged. From this perspective, the four components of a planar quaternion can also be considered as a set of homogeneous coordinates for a planar displacement.

Quaternion algebra is also used for composing two successive planar displacements. Let $\mathbf{Z}_0, \mathbf{Z}_1$ denote two planar displacements. The composition of two planar displacements $\mathbf{Z}_1$ followed by $\mathbf{Z}_0$ is given by the quaternion product $\mathbf{Z}_0\mathbf{Z}_1$.

2.4 Kinematic Constraints of Planar Open Chain

This section reviews the formulation of kinematic constraints of planar RRR, RRP, RPR, PRR and PRP open chains. This has been referenced from Jin [37].

2.4.1 Planar RRR Open Chain

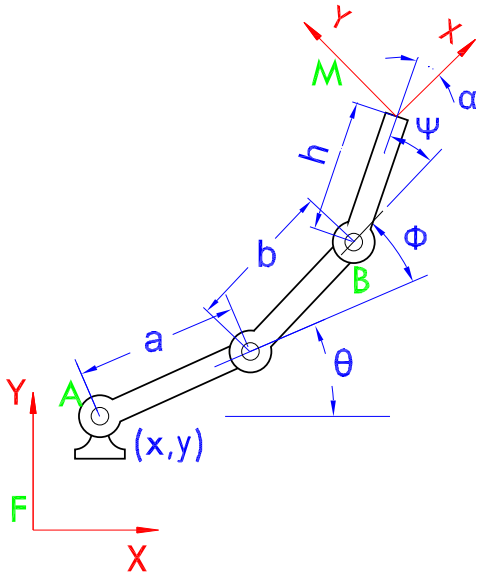

Figure 2.4: A planar 3R open chain.

Consider a planar RRR open chain as shown in Fig. 2.4. The length of the

first link is a, the length of the second link is b and θ, ϕ, ψ are joint angles for three revolute joints respectively. In the figure, **F** and **M** mark the fixed and the moving frames, respectively. The fixed pivot is located at (x, y), while the moving frame is located at a distance of h from the end pivot. The moving frame is assumed to be tilted by angle of α from the line joining the end pivot and the origin of the moving frame. When the fixed and moving frames are located at A and B respectively the parameterized equation of the constraint manifold $\mathbf{Z}(\theta, \phi, \psi)$ of a RRR robot open chain is obtained as follows:

$$\mathbf{Z}(\theta, \phi, \psi) = \mathbf{Z}(\theta)\mathbf{X}(a)\mathbf{Z}(\phi)\mathbf{X}(b)\mathbf{Z}(\psi). \tag{2.7}$$

The coordinates of $\mathbf{Z}(\theta, \phi, \psi) = (Z_1, Z_2, Z_3, Z_4)$ can be obtained as:

$$\begin{aligned} Z_1 &= \frac{a}{2}\cos\frac{\theta - \phi - \psi}{2} + \frac{b}{2}\cos\frac{\theta + \phi - \psi}{2}, \\ Z_2 &= \frac{a}{2}\sin\frac{\theta - \phi - \psi}{2} + \frac{b}{2}\sin\frac{\theta + \phi - \psi}{2}, \\ Z_3 &= \sin\frac{\theta + \phi + \psi}{2}, \\ Z_4 &= \cos\frac{\theta + \phi + \psi}{2}. \end{aligned} \tag{2.8}$$

From Eq. (2.8), it can be seen that the coordinates, Z_i, satisfy the following equations:

$$Z_1^2 + Z_2^2 = a^2/4 + b^2/4 + (ab/2)\cos(\phi). \tag{2.9}$$

$$Z_3^2 + Z_4^2 = 1. \tag{2.10}$$

Since the range of $\cos(\phi)$ is [-1 1], Eq. (2.9) can be reduced to:

$$(a - b)^2/4 \leq Z_1^2 + Z_2^2 \leq (a + b)^2/4. \tag{2.11}$$

The variables θ and ψ can be eliminated from Eq. (2.8) to yield the following equation:

$$4Z_1^2 + 4Z_2^2 - Z_3^2(a^2 + b^2 + 2ab\cos\phi) - Z_4^2(a^2 + b^2 + 2ab\cos\phi) = 0 \quad (2.12)$$

$a^2 + b^2 + 2ab\cos\phi$ is the square of the distance between the base joint and third joint. Let it be denoted by R. Thus the equation becomes

$$Z_1^2 + Z_2^2 - \frac{R^2}{4}Z_3^2 - \frac{R^2}{4}Z_4^2 = 0 \quad (2.13)$$

Let the points of R^4 be denoted x=(x,y,z,w) so the above equation can be written as:

$$x^2 + y^2 - \frac{R^2}{4}z^2 - \frac{R^2}{4}w^2 = 0 \quad (2.14)$$

This can be written in the quadratic form as:

$$x^T[Q]x = 0 \quad (2.15)$$

with the coefficient matrix as:

$$Q = \begin{bmatrix} 1 & 0 & 0 & 0 \\ 0 & 1 & 0 & 0 \\ 0 & 0 & -\frac{R^2}{4} & 0 \\ 0 & 0 & 0 & -\frac{R^2}{4} \end{bmatrix} \quad (2.16)$$

As shown in the Figure 2.4 a general choice of fixed and moving reference planes transforms the coefficient matrix to the form below:

$$[Q'] = [C^{-1}]^T [Q][C^{-1}] \tag{2.17}$$

where, $[C] = [G^+][H^-]$ is the matrix form of the quaternion transformation to the new fixed and moving frames.

$$\begin{aligned} [G] &= (\frac{x}{2}, \frac{y}{2}, 0, 1), \\ [H] &= (\frac{h}{2}\cos\frac{\alpha}{2}, -\frac{h}{2}\sin\frac{\alpha}{2}, \sin\frac{\alpha}{2}, \cos\frac{\alpha}{2}) \end{aligned} \tag{2.18}$$

$$\mathbf{Z}'(\theta, \phi, b)[Q']\mathbf{Z}(\theta, \phi, b) = 0 \tag{2.19}$$

Simplifying the above equation we get:

which gives the following equation:

$$(Z_4^2 - Z_3^2)(\sigma_1 + \sigma_2) + 2Z_3Z_4(\tau_2 - \tau_1) + Z_1Z_3\cos\alpha \tag{2.20}$$

$$-Z_1Z_4 sin\alpha - Z_2Z_3 sin\alpha - Z_2Z_4 cos\alpha = 0$$

Simplifying Eq. (2.20)

$$F(Z_1, Z_2, Z_3, Z_4) = \frac{(Z_1 - \sigma_1 Z_3 - \tau_1 Z_4)^2 + (Z_2 - \sigma_2 Z_3 - \tau_2 Z_4)^2}{Z_3^2 + Z_4^2}, \text{and} \tag{2.21}$$

$$\begin{aligned} \sigma_1 &= (y + h\sin\alpha)/2, & \tau_1 &= (x + h\cos\alpha)/2, \\ \sigma_2 &= (-x + h\cos\alpha)/2, & \tau_2 &= (y - h\sin\alpha)/2. \end{aligned} \tag{2.22}$$

$$\frac{(a-b)^2}{4} \leq F(Z_1, Z_2, Z_3, Z_4) \leq \frac{(a+b)^2}{4}, \tag{2.23}$$

Eq. (2.80) characterize the kinematic constraints of a planar RRR open chain and define the constraint manifold for the chain.

Thus, the constraint manifold of the planar RRR closed chains is given by a pair of concentric and co-oriented sheared hyperboloid and for the a mechanism to pass through a given motion, the image curve would have to be contained within the constraint manifold.

Using the projective property of the planar quaternion, to visualize the hypergeometric shape described by Eq.(2.80), we observe its intersection with the hyperplane $Z_4 = 1$; in the other words, we project Eq.(2.80) onto hyperplane$Z_4 = 1$. Denote $(z_1, z_2, z_3, 1)$ as the projected point of (Z_1, Z_2, Z_3, Z_4), both of which represent the same planar displacement. Then, it is yielded that

$$F(z_1, z_2, z_3, 1) = \frac{(z_1 - \sigma_1 z_3 - \tau_1)^2 + (z_2 - \sigma_2 z_3 - \tau_2)^2}{z_3^2 + 1} \tag{2.24}$$

where σ_1, σ_2, τ_1 and τ_2 are the same as Eq.(2.79).

The volume field described by Eq.(2.24) creates implicit surfaces of (z_1, z_2, z_3). The means to develop the isosurface is to, without loss of generality, set $F(z_1, z_2, z_3, 1) = c$, $c \in [L_{\min}^2/4, L_{\max}^2/4]$, and to be standard, we also reorganize Eq. (2.24) to Eq.(2.25)

$$\frac{(z_1 - \sigma_1 z_3 - \tau_1)^2}{c} + \frac{(z_2 - \sigma_2 z_3 - \tau_2)^2}{c} - z_3^2 = 1 \tag{2.25}$$

This is a typical sheared a circular hyperboloid in the projective (z_1, z_2, z_3) space. See table 2.2. The hyperboloid centralizes at $(\tau_1, \tau_2, 0)$. The central axis is $\frac{z_1 - \tau_1}{\sigma_1} = \frac{z_2 - \tau_2}{\sigma_2} = \frac{z_3}{1}$, so that the hyperboloid orients along the vector$(\sigma_1, \sigma_2, 1)$. It is evident to tell that the center and the orientation are decided by the

Geometric Features	Constraint Parameters
Center	$(\tau_1, \tau_2, 0)$
Orientation	$(\sigma_1, \sigma_2, 1)$
Intersected Circle	$\frac{L_{\min}}{2} \leq r = \sqrt{c} \leq \frac{L_{\max}}{2}$

Table 2.2: Parameters for the projective sheared hyperboloid presented by equation (2.25)

location of the fixed pivot, the length of the floating link and the relative angle of $\mathbf{M}$ to the floating link. Besides, the intersection circle of the hyperboloid with the plane $z_3 = 0$ has a radius, r, equal to $\sqrt{c}$, which determines the size of the hyperboloid; the greater is c, the larger is the size of the hyperboloid. While the value of $F(z_1, z_2, z_3, 1)$ is varying from the lower boundary to the ceiling, except that the size of the hyperbolic manifold increases correspondingly, the center and the orientation keep stationary.

The implicit surfaces is a set of concentric and co oriented sheared projective hyperboloid. The hyperboloid set occupies the space bounded by an interior and an exterior hyperboloid in the projective image. Eq.(2.25).

2.4.2 Planar RRP Open Chain

Consider a planar RRP open chain as shown in Fig. 2.5. The length of the first link is a, the length of the second link is b and θ and ϕ are joint angles for two revolute joints respectively. The second link is a prismatic joint and will have a maximum and minimum travel denoted by b_1 and b_2. In the figure, $\mathbf{F}$ and $\mathbf{M}$ mark the fixed and the moving frames, respectively. The fixed pivot

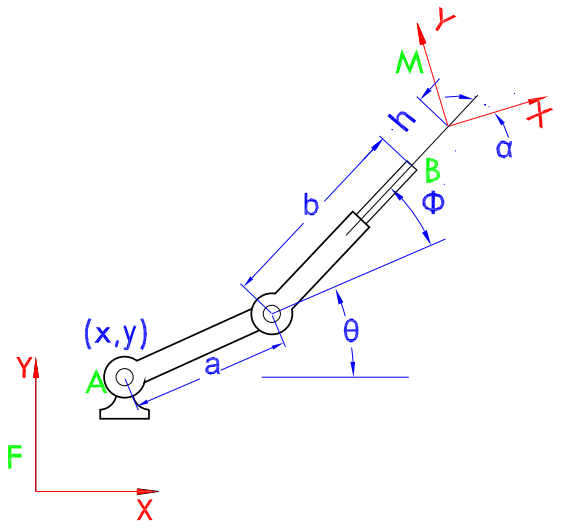

Figure 2.5: A planar RRP open chain.

is located at (x, y), while the moving frame is located at a distance of h from the end pivot. The moving frame is assumed to be tilted by angle of α from the line joining the end pivot and the origin of the moving frame. When the fixed and moving frames are located at A and B respectively the parameterized equation of the constraint manifold $\mathbf{Z}(\theta, \phi, b)$ of a RRP open chain is obtained as follows:

The planar quaternion associated with the end link is given by

$$\mathbf{Z}(\theta, \phi, b) = \mathbf{Z}(\theta)\mathbf{Z}(\phi)\mathbf{X}(b), \tag{2.26}$$

where $\mathbf{Z}(\theta, \phi, b) = (Z_1, Z_2, Z_3, Z_4)$ are

$$\begin{aligned} Z_1 &= \frac{b}{2}\cos\frac{\theta+\phi}{2} + \frac{a}{2}\cos\frac{\theta-\phi}{2}, \\ Z_2 &= \frac{b}{2}\sin\frac{\theta+\phi}{2} + \frac{a}{2}\sin\frac{\theta-\phi}{2}, \\ Z_3 &= \sin\frac{\theta+\phi}{2}, \\ Z_4 &= \cos\frac{\theta+\phi}{2}. \end{aligned} \tag{2.27}$$

It is clear from the above equation that the components of the planar quaternion must satisfy the algebraic equation:

$$(Z_1 - \frac{b}{2}Z_4)^2 + (Z_2 - \frac{b}{2}Z_3)^2 = \frac{a^2}{4}. \tag{2.28}$$

Eq.(2.29) and the range of b ($b_1 \leq b \leq b_2$) guarantee the motion is within workspace.

The Eq. 2.26 can be simplified as:

$$Z_1 Z_3 - Z_2 Z_4 = \frac{a}{2}\sin\phi \tag{2.29}$$

This can be written in the quadratic form as:

$$x^T[Q]x = 0 \tag{2.30}$$

with the coefficient matrix as:

$$Q = \begin{bmatrix} 0 & 0 & 1/2 & 0 \\ 0 & 0 & 0 & -1/2 \\ 1/2 & 0 & 0 & 0 \\ 0 & -1/2 & 0 & 0 \end{bmatrix} \tag{2.31}$$

As shown in the Figure 2.5 a general choice of fixed and moving reference planes transforms the coefficient matrix to the form below:

$$[Q'] = [C^{-1}]^T [Q][C^{-1}] \tag{2.32}$$

where, $[C] = [G^+][H^-]$ is the matrix form of the quaternion transformation to the new fixed and moving frames.

$$\begin{aligned} [G] &= (\frac{x}{2}, \frac{y}{2}, 0, 1), \\ [H] &= (\frac{h}{2}\cos\frac{\alpha}{2}, -\frac{h}{2}\sin\frac{\alpha}{2}, \sin\frac{\alpha}{2}, \cos\frac{\alpha}{2}) \end{aligned} \tag{2.33}$$

$$\mathbf{Z}'(\theta, \phi, b)[Q']\mathbf{Z}(\theta, \phi, b) = C \tag{2.34}$$

where C = constant

Simplifying the above equation we get:

$$(Z_4^2 - Z_3^2)(\sigma_1 + \sigma_2) + 2Z_3Z_4(\tau_2 - \tau_1) + Z_1Z_3\cos\alpha \tag{2.35}$$

$$-Z_1Z_4 sin\alpha - Z_2Z_3 sin\alpha - Z_2Z_4 cos\alpha = C$$

where

$$\begin{aligned} \sigma_1 &= x\sin\alpha, \qquad \tau_1 = y\sin\alpha, \\ \sigma_2 &= y\cos\alpha, \qquad \tau_2 = x\cos\alpha. \end{aligned}$$

Equation(2.35) represents a hyperbolic paraboloid(Refer [46]).

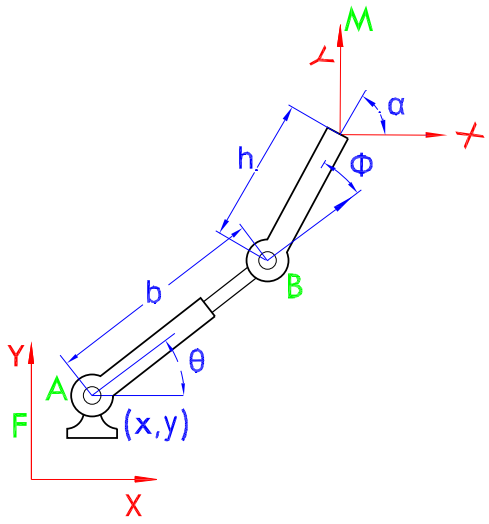

Figure 2.6: A planar RPR open chain.

2.4.3 Planar RPR Open Chain

Consider a planar RPR open chain as shown in Fig. 2.6. The length of the first link is b and θ and ϕ are joint angles for two revolute joints respectively. In the figure, **F** and **M** mark the fixed and the moving frames, respectively. The fixed pivot is located at (x, y), while the moving frame is located at a distance of h from the end pivot. The moving frame is assumed to be tilted by angle of α from the line joining the end pivot and the origin of the moving frame.When the fixed and moving frames are located at A and B respectively the parameterized equation of the constraint manifold $\mathbf{Z}(\theta, b, \phi)$ of a RPR open chain is obtained as follows:

$$\mathbf{Z}(\theta, b, \phi) = \mathbf{Z}(\theta)\mathbf{X}(b)\mathbf{Z}(\phi). \tag{2.36}$$

The coordinates of $\mathbf{Z}(\theta, \phi, \psi) = (Z_1, Z_2, Z_3, Z_4)$ can be obtained as:

$$\begin{aligned} Z_1 &= \frac{b}{2} \cos \frac{\theta - \phi}{2}, \\ Z_2 &= \frac{b}{2} \sin \frac{\theta - \phi}{2}, \\ Z_3 &= \sin \frac{\theta + \phi}{2}, \\ Z_4 &= \cos \frac{\theta + \phi}{2}. \end{aligned} \tag{2.37}$$

From Eq. (2.37), it can be seen that the coordinates, Z_i, satisfy the following equations:

$$Z_1^2 + Z_2^2 = b^2/4 \tag{2.38}$$

$$Z_3^2 + Z_4^2 = 1. \tag{2.39}$$

Eq. (2.38) we get:

$$b_1^2/4 \leq Z_1^2 + Z_2^2 = b^2/4 \leq b_2^2/4. \tag{2.40}$$

This can be written in the quadratic form as:

$$x^T[Q]x = 0 \tag{2.41}$$

with the coefficient matrix as:

$$Q = \begin{bmatrix} 1 & 0 & 0 & 0 \\ 0 & 1 & 0 & 0 \\ 0 & 0 & 0 & 0 \\ 0 & 0 & 0 & 0 \end{bmatrix} \tag{2.42}$$

As shown in the Figure 2.6 a general choice of fixed and moving reference planes transforms the coefficient matrix to the form below:

$$[Q'] = [C^{-1}]^T [Q][C^{-1}] \tag{2.43}$$

where, $[C] = [G^+][H^-]$ is the matrix form of the quaternion transformation to the new fixed and moving frames.

$$\begin{aligned} [G] &= (\frac{x}{2}, \frac{y}{2}, 0, 1), \\ [H] &= (\frac{h}{2}\cos\frac{\alpha}{2}, -\frac{h}{2}\sin\frac{\alpha}{2}, \sin\frac{\alpha}{2}, \cos\frac{\alpha}{2}) \end{aligned} \tag{2.44}$$

$$\mathbf{Z}'(\theta, \phi, b)[Q']\mathbf{Z}(\theta, \phi, b) = 0 \tag{2.45}$$

Simplifying the above equation we get:

$$\begin{aligned} &(Z_4^2 - Z_3^2)(\sigma_1 + \sigma_2) + 2Z_3Z_4(\tau_2 - \tau_1) + Z_1Z_3\cos\alpha \\ &-Z_1Z_4 sin\alpha - Z_2Z_3 sin\alpha - Z_2Z_4 cos\alpha = b^2/4 \end{aligned} \tag{2.46}$$

Simplifying Eq. (2.46)

$$F(Z_1, Z_2, Z_3, Z_4) = \frac{(Z_1 - \sigma_1 Z_3 - \tau_1 Z_4)^2 + (Z_2 - \sigma_2 Z_3 - \tau_2 Z_4)^2}{Z_3^2 + Z_4^2}, \text{and} \tag{2.47}$$

$$\begin{aligned} \sigma_1 &= (y + h\sin\alpha)/2, & \tau_1 &= (x + h\cos\alpha)/2, \\ \sigma_2 &= (-x + h\cos\alpha)/2, & \tau_2 &= (y - h\sin\alpha)/2. \end{aligned} \tag{2.48}$$

$$\frac{b_1^2}{4} \leq F(Z_1, Z_2, Z_3, Z_4) \leq \frac{b_2^2}{4}, \tag{2.49}$$

Eq. (2.49) characterize the kinematic constraints of a planar RPR open chain and define the constraint manifold for the chain.

Thus, the constraint manifold of the planar RPR closed chains is given by a pair of concentric and co-oriented sheared hyperboloid and for the a mechanism to pass through a given motion, the image curve would have to be contained within the constraint manifold.

Using the projective property of the planar quaternion, to visualize the hypergeometric shape described by Eq.(2.49), we observe its intersection with the hyperplane $Z_4 = 1$; in the other words, we project Eq.(2.80) onto hyperplane$Z_4 = 1$. Denote $(z_1, z_2, z_3, 1)$ as the projected point of (Z_1, Z_2, Z_3, Z_4), both of which represent the same planar displacement. Then, it is yielded that

$$F(z_1, z_2, z_3, 1) = \frac{(z_1 - \sigma_1 z_3 - \tau_1)^2 + (z_2 - \sigma_2 z_3 - \tau_2)^2}{z_3^2 + 1} \tag{2.50}$$

where σ_1, σ_2, τ_1 and τ_2 are the same as Eq.(2.48).

The volume field described by Eq.(2.50) creates implicit surfaces of (z_1, z_2, z_3). The means to develop the isosurface is to, without loss of generality, set $F(z_1, z_2, z_3, 1) = c$, $c \in [L_{\min}^2/4, L_{\max}^2/4]$, and to be standard, we also reorganize Eq. (2.50);

$$\frac{(z_1 - \sigma_1 z_3 - \tau_1)^2}{c} + \frac{(z_2 - \sigma_2 z_3 - \tau_2)^2}{c} - z_3^2 = 1 \tag{2.51}$$

This is a typical sheared a circular hyperboloid in the projective (z_1, z_2, z_3) space. See table 3.1. The hyperboloid centralizes at $(\tau_1, \tau_2, 0)$. The central axis is $\frac{z_1 - \tau_1}{\sigma_1} = \frac{z_2 - \tau_2}{\sigma_2} = \frac{z_3}{1}$, so that the hyperboloid orients along the vector$(\sigma_1, \sigma_2, 1)$. It is evident to tell that the center and the orientation are decided by the location of the fixed pivot, the length of the floating link and the relative angle of $\mathbf{M}$ to the floating link. Besides, the intersection circle of the hyperboloid

Geometric Features	Constraint Parameters
Center	$(\tau_1, \tau_2, 0)$
Orientation	$(\sigma_1, \sigma_2, 1)$
Intersected Circle	$\frac{L_{\min}}{2} \leq r = \sqrt{c} \leq \frac{L_{\max}}{2}$

Table 2.3: Parameters for the projective sheared hyperboloid presented by equation (2.51)

with the plane $z_3 = 0$ has a radius, r, equal to $\sqrt{c}$, which determines the size of the hyperboloid; the greater is c, the larger is the size of the hyperboloid. While the value of $F(z_1, z_2, z_3, 1)$ is varying from the lower boundary to the ceiling, except that the size of the hyperbolic manifold increases correspondingly, the center and the orientation keep stationary.

As a matter of fact, the implicit surfaces is a set of concentric and co oriented sheared projective hyperboloid. The hyperboloid set occupies the space bounded by an interior and an exterior hyperboloid in the projective image. Eq.(2.51) and Table 2.3 introduce how the the shape of the hyperboloid set is influenced by the configuration of the open chain.

2.4.4 Planar PRR Open Chain

Consider a planar PRR open chain as shown in Fig. 2.7. The length of the first link is b, the length of the second link is a and θ and ϕ are joint angles for two revolute joints respectively. The first link is a prismatic joint and will have a maximum and minimum travel denoted by b_1 and b_2. In the figure, **F** and **M** mark the fixed and the moving frames, respectively. The fixed pivot is located

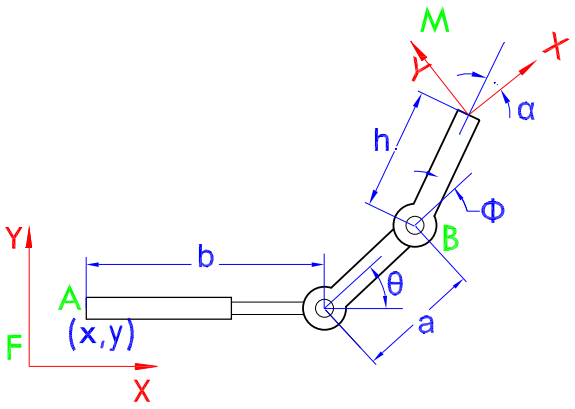

Figure 2.7: A planar PRR open chain.

at (x, y), while the moving frame is located at a distance of h from the end pivot. The moving frame is assumed to be tilted by angle of α from the line joining the end pivot and the origin of the moving frame. When the fixed and moving frames are located at A and B respectively the parameterized equation of the constraint manifold $\mathbf{Z}(b, \theta, \phi)$ of a PRR robot open chain is obtained as follows:

The planar quaternion for the end link is given by

$$\mathbf{Z}(b, \theta, \phi) = \mathbf{X}(b)\mathbf{Z}(\theta)\mathbf{Z}(\phi), \tag{2.52}$$

where

$$\begin{aligned} Z_1 &= \frac{a}{2}\cos\frac{\theta-\phi}{2} + \frac{b}{2}\cos\frac{\theta+\phi}{2}, \\ Z_2 &= \frac{a}{2}\sin\frac{\theta-\phi}{2} - \frac{b}{2}\sin\frac{\theta+\phi}{2}, \\ Z_3 &= \sin\frac{\theta+\phi}{2}, \\ Z_4 &= \cos\frac{\theta+\phi}{2}. \end{aligned} \tag{2.53}$$

Thus the kinematic constraint associated with the PRR chain is given by

$$\begin{array}{c}(Z_1 - \frac{b}{2})^2 + (Z_2 + \frac{b}{2}Z_3)^2 = \frac{a^2}{4}, \\ b_1 \leq b \leq b_2.\end{array} \tag{2.54}$$

The Eq. 2.53 can be simplified as:

$$Z_1 Z_3 - Z_2 Z_4 = \frac{a}{2}\sin\theta \tag{2.55}$$

This can be written in the quadratic form as:

$$x^T[Q]x = C \tag{2.56}$$

with the coefficient matrix as:

$$Q = \begin{bmatrix} 0 & 0 & 1/2 & 0 \\ 0 & 0 & 0 & 1/2 \\ 1/2 & 0 & 0 & 0 \\ 0 & 1/2 & 0 & 0 \end{bmatrix} \tag{2.57}$$

As shown in the Figure 2.7 a general choice of fixed and moving reference planes transforms the coefficient matrix to the form below:

$$[Q'] = [C^{-1}]^T[Q][C^{-1}] \tag{2.58}$$

where, $[C] = [G^+][H^-]$ is the matrix form of the quaternion transformation to the new fixed and moving frames.

$$\begin{aligned}[G] &= (\frac{x}{2}, \frac{y}{2}, 0, 1), \\ [H] &= (\frac{h}{2}\cos\frac{\alpha}{2}, -\frac{h_1}{2}\sin\frac{\alpha}{2}, \sin\frac{\alpha}{2}, \cos\frac{\alpha}{2})\end{aligned} \tag{2.59}$$

$$\mathbf{Z}'(\theta, \phi, b)[Q']\mathbf{Z}(\theta, \phi, b) = C \tag{2.60}$$

where C = constant

Simplifying the above equation we get:

$$-\frac{Z_3^2}{2}(y + hsin\alpha) - \frac{Z_4^2}{2}(y - hsin\alpha) - Z_3 Z_4 h_1 cos\alpha + Z_1 Z_3 + Z_4 Z_2 = C \tag{2.61}$$

Equation(2.61) represents a hyperbolic paraboloid(Refer [46]).

2.4.5 Planar PRP Open Chain

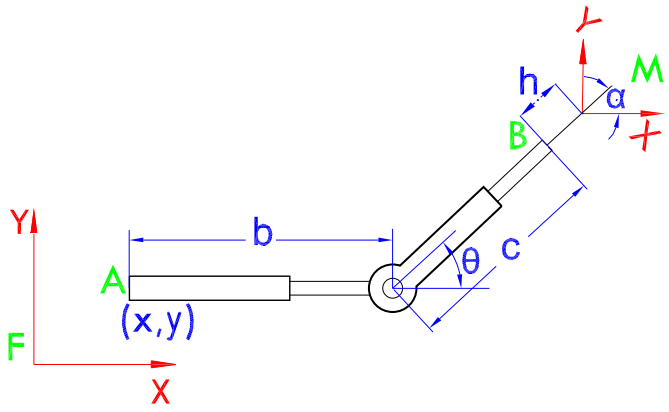

Figure 2.8: A planar PRP open chain.

Consider a planar PRP open chain as shown in Fig. 2.8. The length of the first link is b, the length of the second link is c and θ and is the joint angles of the revolute joint. The first link is a prismatic joint and will have a maximum and minimum travel denoted by b_1 and b_2. In the figure, **F** and **M** mark the fixed and the moving frames, respectively. The fixed pivot is located at (x, y), while the moving frame is located at a distance of h from the end pivot. The

moving frame is assumed to be tilted by angle of α from the line joining the end pivot and the origin of the moving frame. When the fixed and moving frames are located at A and B respectively the parameterized equation of the constraint manifold $\mathbf{Z}(b, \theta, c)$ of a PRP open chain is obtained as follows:

The planar quaternion for the end link is given by

$$\mathbf{Z}(b, \theta, c) = \mathbf{X}(b)\mathbf{Z}(\theta)\mathbf{X}(c). \tag{2.62}$$

where

$$\begin{aligned} Z_1 &= \frac{b+c}{2}\cos\frac{\theta}{2}, \\ Z_2 &= \frac{c-b}{2}\sin\frac{\theta}{2}, \\ Z_3 &= \sin\frac{\theta}{2}, \\ Z_4 &= \cos\frac{\theta}{2}. \end{aligned} \tag{2.63}$$

The kinematic constraints for the chain are given by

$$\begin{aligned} &Z_1 = \tfrac{b+c}{2} Z_4, \\ &Z_2 = \tfrac{c-b}{2} Z_3, \\ &b_1 \leq b \leq b_2, \\ &c_1 \leq c \leq c_2. \end{aligned} \tag{2.64}$$

The Eq. 2.63 can be simplified as:

$$Z_1 Z_3 + Z_2 Z_4 - c Z_3 Z_4 = 0 \tag{2.65}$$

This can be written in the quadratic form as:

$$x^T [Q] x = 0 \tag{2.66}$$

with the coefficient matrix as:

$$Q = \begin{bmatrix} 0 & 0 & 1/2 & 0 \\ 0 & 0 & 0 & 1/2 \\ 1/2 & 0 & 0 & -c/2 \\ 0 & 1/2 & -c/2 & 0 \end{bmatrix} \tag{2.67}$$

As shown in the Figure 2.7 a general choice of fixed and moving reference planes transforms the coefficient matrix to the form below:

$$[Q'] = [C^{-1}]^T [Q][C^{-1}] \tag{2.68}$$

where, $[C] = [G^+][H^-]$ is the matrix form of the quaternion transformation to the new fixed and moving frames.

$$\begin{aligned} [G] &= (\frac{x}{2}, \frac{y}{2}, 0, 1), \\ [H] &= (\frac{h}{2}\cos\frac{\alpha}{2}, -\frac{h}{2}\sin\frac{\alpha}{2}, \sin\frac{\alpha}{2}, \cos\frac{\alpha}{2}) \end{aligned} \tag{2.69}$$

$$\mathbf{Z}'(\theta, \phi, b)[Q']\mathbf{Z}(\theta, \phi, b) = 0 \tag{2.70}$$

Simplifying the above equation we get:

$$\begin{aligned} -Z_3^2\frac{(y + hsin\alpha + csin\alpha)}{2} + Z_4^2\frac{(-y + hsin\alpha + csin\alpha)}{2} \\ -Z_3Z_4(hcos\alpha + ccos\alpha) + Z_3Z_1 + Z_4Z_2 = C \end{aligned} \tag{2.71}$$

where,

C = constant.

Equation(2.71) represents a hyperbolic paraboloid(Refer [46]).

2.5 Kinematic Constraints of Planar Parallel Manipulator

This section reviews the formulation of the kinematic constraints of a planar parallel manipulator.

A three legged planar parallel manipulator made up of RRR, RPR and RRR chains is considered in this case. Thus as explained in Section 2.4 the kinematic constraint equation of a planar parallel manipulator will be the combination of the kinematic constraint equation of all the three types of open chains connected.

First Open Chain (RRR)

$$F_1(Z_1, Z_2, Z_3, Z_4) = \frac{(Z_1 - \sigma_1 Z_3 - \tau_1 Z_4)^2 + (Z_2 - \sigma_2 Z_3 - \tau_2 Z_4)^2}{Z_3^2 + Z_4^2}, \text{and} \quad (2.72)$$

$$\begin{aligned} \sigma_1 &= (y + h\sin\alpha)/2, & \tau_1 &= (x + h\cos\alpha)/2, \\ \sigma_2 &= (-x + h\cos\alpha)/2, & \tau_2 &= (y - h\sin\alpha)/2. \end{aligned} \quad (2.73)$$

$$\frac{(a-b)^2}{4} \leq F_1(Z_1, Z_2, Z_3, Z_4) \leq \frac{(a+b)^2}{4}, \quad (2.74)$$

Second Open Chain (RPR)

$$F_2(Z_1, Z_2, Z_3, Z_4) = \frac{(Z_1 - \sigma_1 Z_3 - \tau_1 Z_4)^2 + (Z_2 - \sigma_2 Z_3 - \tau_2 Z_4)^2}{Z_3^2 + Z_4^2}, \text{and} \quad (2.75)$$

$$\begin{aligned} \sigma_1 &= (y + h\sin\alpha)/2, & \tau_1 &= (x + h\cos\alpha)/2, \\ \sigma_2 &= (-x + h\cos\alpha)/2, & \tau_2 &= (y - h\sin\alpha)/2. \end{aligned} \quad (2.76)$$

$$\frac{(a-b)^2}{4} \leq F_2(Z_1, Z_2, Z_3, Z_4) \leq \frac{(a+b)^2}{4}, \quad (2.77)$$

Third Open Chain (RRR)

$$F_3(Z_1, Z_2, Z_3, Z_4) = \frac{(Z_1 - \sigma_1 Z_3 - \tau_1 Z_4)^2 + (Z_2 - \sigma_2 Z_3 - \tau_2 Z_4)^2}{Z_3^2 + Z_4^2}, \text{and} \quad (2.78)$$

$$\begin{array}{ll} \sigma_1 = (y + h\sin\alpha)/2, & \tau_1 = (x + h\cos\alpha)/2, \\ \sigma_2 = (-x + h\cos\alpha)/2, & \tau_2 = (y - h\sin\alpha)/2. \end{array} \quad (2.79)$$

$$\frac{(a-b)^2}{4} \leq F_3(Z_1, Z_2, Z_3, Z_4) \leq \frac{(a+b)^2}{4}, \quad (2.80)$$

As explained in section 2.4.1 and section 2.4.3 the kinematic constraint equations represent a set of concentric and co-oriented sheared hyperboloid. Thus in this case there will be three sets of hyperboloids.

Chapter 3

Kinematic Constraints of Spherical Mechanisms

3.1 Introduction

This chapter deals with the formulation of kinematic constraints of spherical mechanisms using quaternion based representation found in McCarthy [35] and Ge [36].

The organization of this chapter is as follows. Section 3.2 explains the spherical displacements and quaternions. Section 3.3 presents the constraint manifolds of spherical 3R open chains and Section 3.4 presents the constraint manifolds of 6R closed chains.

3.2 Spherical Displacements and Quaternions

The rotation of a three dimensional body, $\mathbf{M}$, with respect to a fixed body, $\mathbf{F}$, can be viewed as a displacement of the frame $\mathbf{M}$ from an initial position coinciding with $\mathbf{F}$ to its final position. Let $\mathbf{x}$ and $\mathbf{X}$ be three dimensional vectors

defining coordinates of a point P in $\mathbf{M}$ and $\mathbf{F}$, then under this displacement the point P is constrained to lie on a sphere and this displacement is termed a *spherical displacement*.

Any rotation in three-dimensional space has a rotation axis and a rotation angle about this axis. Let $\mathbf{s} = (s_x, s_y, s_z)$ denote a unit vector along the axis and θ denote the angle of rotation. They can be used to define the so-called *Euler-Rodrigues parameters:*

$$q_1 = s_x \sin(\theta/2),\ q_2 = s_y \sin(\theta/2),\ q_3 = s_z \sin(\theta/2),\ q_4 = \cos(\theta/2). \tag{3.1}$$

The Euler-Rodrigues parameters and the quaternion units, $1, \mathbf{i}, \mathbf{j}, \mathbf{k}$ can be combined to define a quaternion of rotation:

$$\mathbf{q} = q_1\mathbf{i} + q_2\mathbf{j} + q_3\mathbf{k} + q_4. \tag{3.2}$$

A quaternion $\mathbf{q}$, at times, is also written as an ordered quadruple (q_1, q_2, q_3, q_4). Since $q_1^2 + q_2^2 + q_3^2 + q_4^2 = 1$, $\mathbf{q}$ is also called a unit quaternion. Details on quaternions are found in Bottema and Roth [47] and McCarthy [35].

If we consider $\mathbf{x}$ and $\mathbf{X}$ as the *vector quaternions* (no coefficient of 1), then the rotation is given by the quaternion equation

$$\mathbf{X} = \mathbf{q}\mathbf{x}\mathbf{q}^* \tag{3.3}$$

where $\mathbf{q}^* = q_4 - q_1\mathbf{i} - q_2\mathbf{j} - q_3\mathbf{k}$ is the conjugate of $\mathbf{q}$.

We can apply homogeneous transform matrix form to represent the Eq. (3.3):

$$\begin{bmatrix} \mathbf{X} \\ 1 \end{bmatrix} = [A] \begin{bmatrix} \mathbf{x} \\ 1 \end{bmatrix}, \tag{3.4}$$

where

$$[A] = \frac{1}{S^2}\begin{bmatrix} q_4^2+q_1^2-q_2^2-q_3^2 & 2(q_1q_2-q_4q_3) & 2(q_1q_3+q_4q_2) & 0 \\ 2(q_2q_1+q_4q_3) & q_4^2-q_1^2+q_2^2-q_3^2 & 2(q_2q_3-q_4q_1) & 0 \\ 2(q_3q_1-q_4q_2) & 2(q_3q_2+q_4q_1) & q_4^2-q_1^2-q_2^2+q_3^2 & 0 \\ 0 & 0 & 0 & S^2 \end{bmatrix}, \tag{3.5}$$

where $S^2 = q_1^2 + q_2^2 + q_3^2 + q_4^2$.

Note that when q_i is replaced by $Q_i = wq_i$ $(i = 1, 2, 3, 4)$, where w is a nonzero scalar, the matrix $[A]$ is unchanged. Thus, the quaternion components of $\mathbf{q}$ can be considered as homogeneous coordinates of a rotation.

Quaternion algebra is also used for composing two successive rotations. Let $\mathbf{Q}_0, \mathbf{Q}_1$ denote two rotations. The composition of two rotations $\mathbf{Q}_1$ followed by $\mathbf{Q}_0$ is given by the quaternion product $\mathbf{Q}_0\mathbf{Q}_1$.

3.3 Kinematic Constraints of Spherical Open Chain

This section reviews the formulation of kinematic constraints of spherical 3R open chain which can be found in Jin [37]

3.3.1 Spherical 3R Open Chain

Consider a spherical 3R open chain (see Figure 3.1) with joint axes **a, b, c** intersecting a fixed point O. The axes **a, b** make an angle α and **b, c** make an angle β. We attach a fixed frame **O** to O and moving frames **A, B, C** to each links. The joint angles are denoted as θ, ϕ, and ψ for the successive joints. For details on the orientation of the moving frames, we again refer the reader

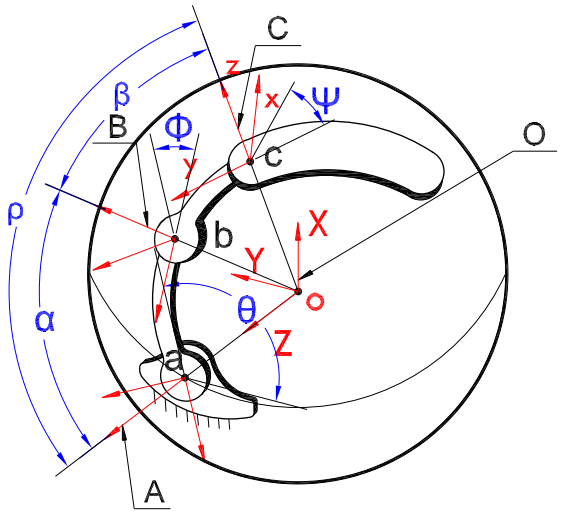

Figure 3.1: A spherical 3R open chain.

to McCarthy [35]. The orientation of the end link is given by the following quaternion product:

$$\mathbf{q}(\theta, \phi, \psi) = \mathbf{Z}(\theta)\mathbf{X}(\alpha)\mathbf{Z}(\phi)\mathbf{X}(\beta)\mathbf{Z}(\psi), \tag{3.6}$$

where,

$$\begin{array}{l} \mathbf{Z}(\theta) = (0, 0, \sin(\theta/2), \cos(\theta/2)), \\ \mathbf{X}(\alpha) = (\sin(\alpha/2), 0, 0, \cos(\alpha/2)), \\ \mathbf{Z}(\phi) = (0, 0, \sin(\phi/2), \cos(\phi/2)), \\ \mathbf{X}(\beta) = (\sin(\beta/2), 0, 0, \cos(\beta/2)), \\ \mathbf{Z}(\psi) = (0, 0, \sin(\psi/2), \cos(\psi/2)). \end{array} \tag{3.7}$$

By expanding the product in Eq. (3.6) we obtain $\mathbf{q}(\theta, \phi, \psi) = (q_1, q_2, q_3, q_4)$, where

$$\begin{array}{l} q_1 = \cos(\frac{\phi}{2})\sin(\frac{\alpha+\beta}{2})\cos(\frac{\theta-\psi}{2}) + \sin(\frac{\phi}{2})\sin(\frac{\alpha-\beta}{2})\sin(\frac{\theta-\psi}{2}), \\ q_2 = \cos(\frac{\phi}{2})\sin(\frac{\alpha+\beta}{2})\sin(\frac{\theta-\psi}{2}) - \sin(\frac{\phi}{2})\sin(\frac{\alpha-\beta}{2})\cos(\frac{\theta-\psi}{2}), \\ q_3 = \cos(\frac{\phi}{2})\cos(\frac{\alpha+\beta}{2})\sin(\frac{\theta+\psi}{2}) + \sin(\frac{\phi}{2})\cos(\frac{\alpha-\beta}{2})\cos(\frac{\theta+\psi}{2}), \\ q_4 = \cos(\frac{\phi}{2})\cos(\frac{\alpha+\beta}{2})\cos(\frac{\theta+\psi}{2}) - \sin(\frac{\phi}{2})\cos(\frac{\alpha-\beta}{2})\sin(\frac{\theta+\psi}{2}). \end{array} \tag{3.8}$$

Equation (3.8) further gives:

$$\begin{aligned} q_1^2 + q_2^2 &= \cos^2(\tfrac{\phi}{2})\sin^2(\tfrac{\alpha+\beta}{2}) + \sin^2(\tfrac{\phi}{2})\sin^2(\tfrac{\alpha-\beta}{2}), \\ q_3^2 + q_4^2 &= \cos^2(\tfrac{\phi}{2})\cos^2(\tfrac{\alpha+\beta}{2}) + \sin^2(\tfrac{\phi}{2})\cos^2(\tfrac{\alpha-\beta}{2}). \end{aligned} \tag{3.9}$$

Since α, β satisfy the condition $0 < \alpha, \beta < \pi$, Eq. (3.9) reduces to the following inequality:

$$\tan^2((\alpha-\beta)/2) \leq \frac{q_1^2 + q_2^2}{q_3^2 + q_4^2} \leq \tan^2((\alpha+\beta)/2). \tag{3.10}$$

This inequality characterizes the kinematic constraint of a spherical 3R open chain. The Eq. (3.10) is equivalent to:

$$\sin^2((\alpha-\beta)/2) \leq \frac{q_1^2 + q_2^2}{q_1^2 + q_2^2 + q_3^2 + q_4^2} \leq \sin^2((\alpha+\beta)/2), \tag{3.11}$$

or

$$\cos^2((\alpha+\beta)/2) \leq \frac{q_3^2 + q_4^2}{q_1^2 + q_2^2 + q_3^2 + q_4^2} \leq \cos^2((\alpha-\beta)/2). \tag{3.12}$$

Note once again that when q_i $(i = 1, 2, 3, 4)$ is replaced by $Q_i = wq_i$, where w is a scalar, Eq. (3.10), (3.11) and (3.12) are unchanged.

3.4 Kinematic Constraints of Spherical Closed Chain

This section reviews the formulation of kinematic constraints of spherical 6R closed chains.

3.4.1 Spherical 6R Closed Chain

In this section, we review the constraint manifolds of spherical 6R closed chains; see McCarthy [35] and Ge [36] for details on constraint manifold. The

kinematic constraints of the spherical closed chains specify the positions and orientations obtainable by a certain link of the chain. The interest here is in the coupler of the chain.

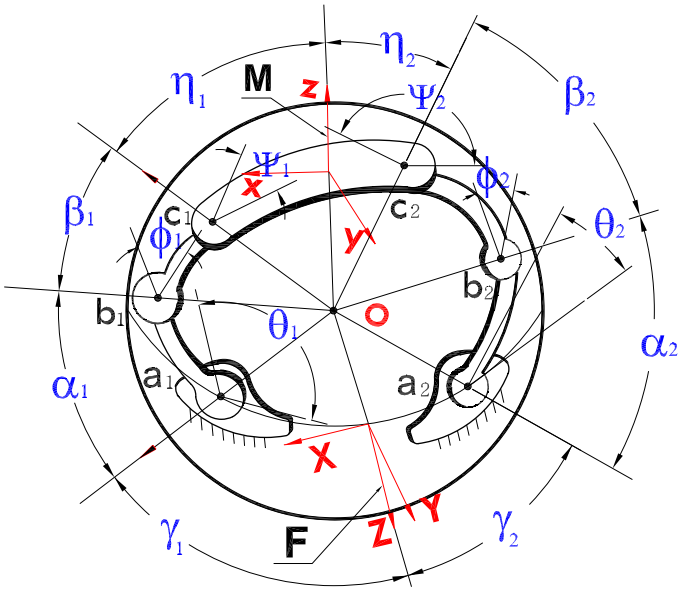

Figure 3.2: A 6R Spherical closed chain

Consider a spherical 6R closed chain (see Figure 3.2), with moving pivots attached to the coupler at $\mathbf{c}_1$ and $\mathbf{c}_2$, and fixed pivots are located at $\mathbf{a}_1$ and $\mathbf{a}_2$. The joint axes at all the pivots intersect at a fixed point $\mathbf{O}$, the center of the design sphere. The fixed frame $\mathbf{F}(\mathbf{XYZ})$ is located on the great circular arc joining the two fixed pivots. The angle between the fixed pivot $\mathbf{a}_1$ and the fixed frame is denoted by γ_1, while between $\mathbf{a}_2$ and the fixed frame is denoted by γ_2. The fixed frame is oriented such that its X-axis is normal to the plane defined by $\mathbf{O}$ and the fixed pivots $\mathbf{a}_1$, $\mathbf{a}_2$ in the direction $(\mathbf{a}_1 - \mathbf{O}) \times (\mathbf{a}_2 - \mathbf{O})$, while The Z-axis points away from the center of the sphere $\mathbf{O}$ to the origin

of the frame. Similarly, the moving frame **M** (**xyz**) is positioned on the great circular arc joining the moving pivots, and is at a distance of η_1 and η_2 from the moving pivots $\mathbf{c}_1$ and $\mathbf{c}_2$, respectively. Similar to the orientation of the fixed frame, its x-axis is normal to the plane defined by the moving joints $\mathbf{c}_1$ and $\mathbf{c}_2$ in the direction $(\mathbf{c}_1 - \mathbf{O}) \times (\mathbf{c}_2 - \mathbf{O})$ and the z-axis points along the vector joining from $\mathbf{O}$ to the origin of the frame.

A spherical 6R closed chain can be seen as two 3R open chains joined together at the ends. The joint angles for the first and the second 3R open chain are denoted θ_1, ϕ_1, ψ_1 and θ_2, ϕ_2, ψ_2, respectively, while the angular length of the links joining the coupler are $\alpha_1, \beta_1, \alpha_2$, and β_2. Then, the constraint manifold for the spherical 6R closed chain is the intersection of constraint manifold of the left and the right spherical 3R open chains. If the displacement of the moving object attached to the moving frame is represented by a quaternion $Q = (Y_1, Y_2, Y_3, Y_4)$, then after eliminating the joint angles from the forward kinematics of each open chain (see McCarthy [35] or Purwar et al. [32]), the algebraic equations for the two manifolds are given by:

Left 3R open chain:

$$\cos^2(\frac{\alpha_1 + \beta_1}{2}) \leq F_1(Y_1, Y_2, Y_3, Y_4) \leq \cos^2(\frac{\beta_1 - \alpha_1}{2}), \tag{3.13}$$

where

$$F_1(Y_1, Y_2, Y_3, Y_4) = \frac{(Y_1 \sin\tau_1 - Y_4 \cos\tau_1)^2 + (Y_2 \sin\sigma_1 + Y_3 \cos\sigma_)^2}{Y_1^2 + Y_2^2 + Y_3^2 + Y_4^2}, \tag{3.14}$$

and

$$\sigma_1 = (\gamma_1 + \eta_1)/4, \tau_1 = (\gamma_1 - \eta_1)/4. \tag{3.15}$$

Right 3R open chain:

$$\cos^2(\frac{\alpha_2+\beta_2}{2}) \leq F_2(Y_1,Y_2,Y_3,Y_4) \leq \cos^2(\frac{\beta_2-\alpha_2}{2}), \tag{3.16}$$

where

$$F_2(Y_1,Y_2,Y_3,Y_4) = \frac{(Y_1\sin\tau_2 + Y_4\cos\tau_2)^2 + (Y_2\sin\sigma_2 - Y_3\cos\sigma_2)^2}{Y_1^2+Y_2^2+Y_3^2+Y_4^2}, \tag{3.17}$$

and

$$\sigma_2 = (\gamma_2+\eta_2)/4, \tau_2 = (\gamma_2-\eta_2)/4. \tag{3.18}$$

Equations (3.13) and (3.16) characterize the kinematic constraints of a spherical 6R closed chain and are said to define the constraint manifold for the spherical 6R closed chain (McCarthy [35]).

To visualize the hypergeometric shape described by Eq.(3.13) or (3.16), we observe its projection on the hyperplane $Y_4 = 1$. Denote $(y_1, y_2, y_3, 1)$ as the projected point of (Y_1, Y_2, Y_3, Y_4), both of which represent the same spherical displacement. Then, $F_1(Y_1, Y_2, Y_3, Y_4)$ on $Y_4 = 1$ after some algebraic rearrangement is given by

$$\frac{[y_1 - \frac{\sin\tau_1\cos\tau_1}{\sin^2\tau_1 - c}]^2}{\frac{c-c^2}{(\sin^2\tau_1-c)^2}} + \frac{[y_2 + \frac{\sin\sigma_1\cos\sigma_1}{\sin^2\sigma_1-c}y_3]^2}{\frac{c-c^2}{(\sin^2\sigma_1-c)(\sin^2\tau_1-c)}} - \frac{y_3^2}{\frac{\sin^2\sigma_1-c}{\sin^2\tau_1-c}} = 1 \tag{3.19}$$

where

$$\sigma_1 = \frac{-\gamma_1+\eta_1}{2}, \quad \tau_1 = \frac{-\gamma_1-\eta_1}{2} \tag{3.20}$$

and

$$c \in [\cos^2\frac{\alpha_1+\beta_1}{2}, \cos^2\frac{\alpha_1-\beta_1}{2}]. \tag{3.21}$$

Geometric Features	Constraint Parameters
Center	$(\frac{\sin\tau_1\cos\tau_1}{\sin^2\tau_1-c}, 0, 0)$
Orientation	$(0, -\frac{\sin\sigma_1\cos\sigma_1}{\sin^2\sigma_1-c}, 1)$
Intersected ellipse	major radius $= \frac{c-c^2}{(\sin^2\tau-c)^2}$,
	minor radius $= \frac{c-c^2}{(\sin^2\sigma_1-c)(\sin^2\tau_1-c)}$

Table 3.1: Parameters for the projective sheared hyperboloid

Equation (3.19) represents an elliptic hyperboloid with the center given by $(\frac{\sin\tau_1\cos\tau_1}{\sin^2\tau_1-c}, 0, 0)$, and the orientation of the central axis given by vector $(0, -\frac{\sin\sigma_1\cos\sigma_1}{\sin^2\sigma_1-c}, 1)$. It is evident that the center and the orientation are dependent on the location of the fixed pivots and moving pivots, as well as the dimensions of the links. The hyperboloid intersects plane $y_3 = 0$ in an ellipse. When the value of $F_1(y_1, y_2, y_3, 1)$ varies from its minimum to maximum, the size of the manifold increases correspondingly. However, an unintended effect caused by the dependence of the location of the center and the orientation on the size also forces a change in the size of the hyperboloid when either of the center or orientation are varied. Table 3.1 summarizes the relationship between geometric features of the hyperboloid and the mechanism parameters for the left open 3R chains. A similar set of relationship exists for the right open chain as well. Thus, the constraint manifold of the spherical 6R closed chains is given by the intersection of two pairs of sheared elliptic hyperboloids, and for a mechanism to pass through a given motion, the image curve has to be contained within the constraint manifold.

Chapter 4

Interactive Dimensional Synthesis and Motion Design

4.1 Interactive Dimensional Synthesis

The design method treats a 6R closed chain as a mechanism assembled using two independent 3R open chains and a three legged planar parallel manipulator as three independent open chains. The constraint manifold of both the chains are geometric objects in the image space, the size, shape and position of which are a function of mechanism parameters. A given rational motion maps to an image curve that needs to be contained inside these manifolds. This section, describes the procedure required to design a 6R spherical closed chain and a planar parallel manipulator. It also describes the user interface with which the designer needs to be familiar. The basic idea is that the designers are provided with a set of controls via the graphical user interface (GUI) of the tool that will allow them to interactively manipulate the constraint manifold with the objective to contain the image curve in the manifold. Upon being satisfied visually, the designer will be allowed to instruct the program to check if there are any violations of the kinematic constraints.

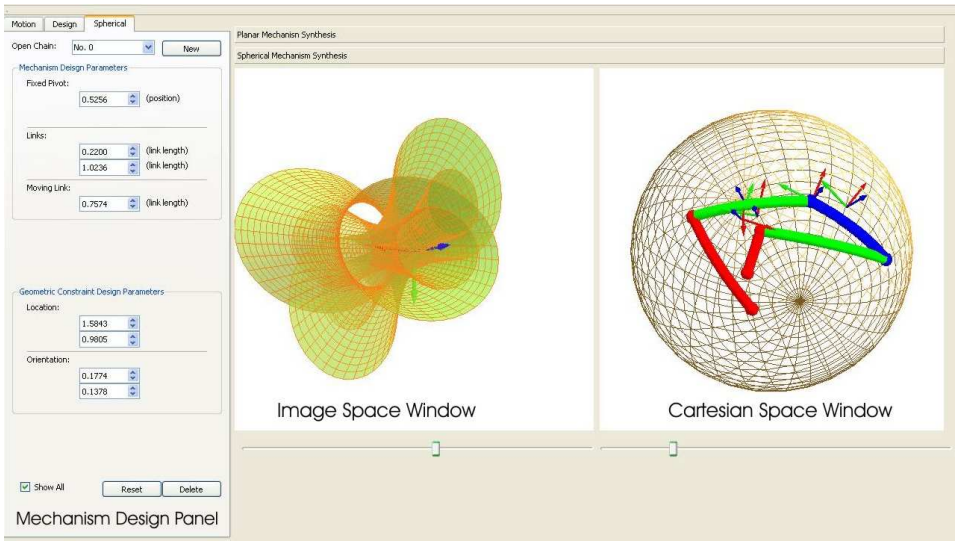

Figure 4.1: A screenshot of the annotated panels and the window space for spherical 6R chain

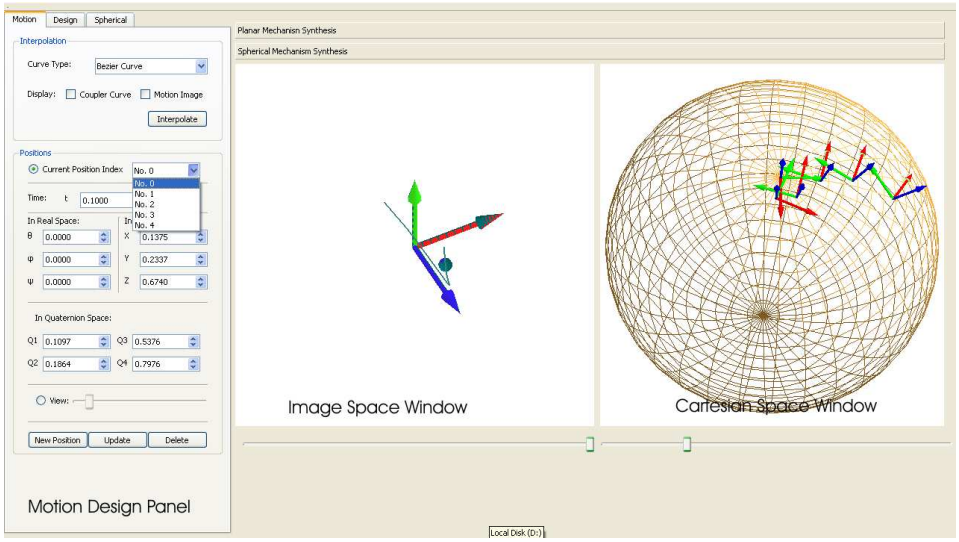

Figure 4.2: Another screenshot of the annotated panels and the window space for spherical 6R chain

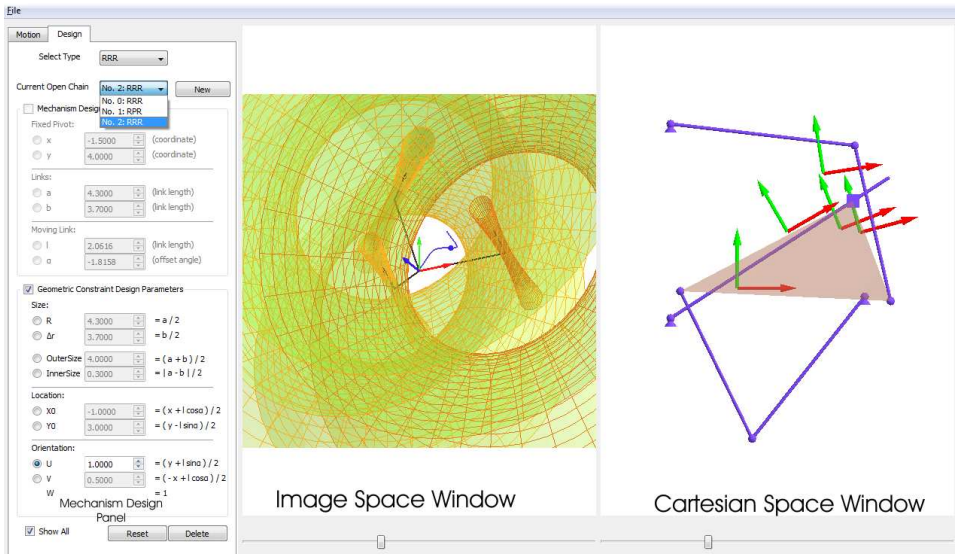

Figure 4.3: A screenshot of the annotated panels and the window space for planar parallel manipulator

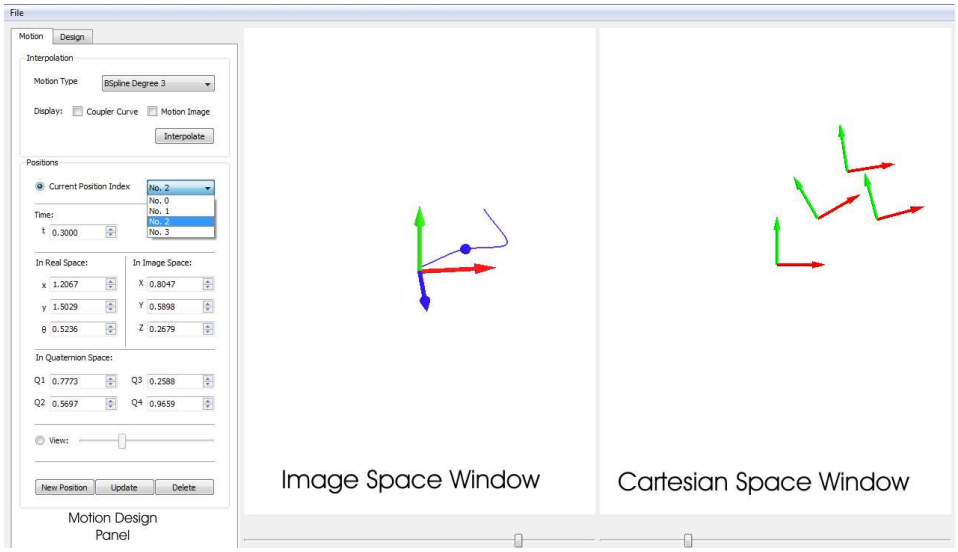

Figure 4.4: Another screenshot of the annotated panels and the window space for planar parallel manipulator

A windows binary of the tool for x86 architecture can be downloaded at `http://cadcam.eng.sunysb.edu/dimsynthspherical/` for the spherical 6R chain and `http://cadcam.eng.sunysb.edu/dimsynthparallel/` for a planar parallel manipulator.

4.1.1 User Interface Functionalities

In terms of functionalities, the GUI has four parts, as shown in Figs. 4.1 and 4.2 for spherical 6R closed chain and Figs. 4.3 and 4.4 for planar parallel manipulator:

1. The Cartesian Space Window (CSW): This window is used to display the given positions, the animation of the mechanism and the open chains in the Cartesian space.

2. The Image Space Window (ISW): In this window, the constraint manifold as well as the image curve projected on the hyperplane are shown.

3. Motion Design Panel (MoDP): This panel supports operations like position insertion, deletion and modification, and comprises of functions to animate the motion and to test for constraint violation. The constraint violation test is done and the test results are visualized through the user interface. This operation updates both the Cartesian Space Window and the Image space Window.

4. Mechanism Design Panel (MeDP): There are two ways to edit the mechanism: 1) directly manipulate mechanism parameters in the Cartesian

space, like the location, the link lengthes and the relative angle, and as a consequence, constraint manifolds change in the image space, or 2) edit the geometric parameters that change the size, position, and the orientation of the manifolds. In case of a planar parallel manipulator the designers may find the latter approach more intuitive. Whereas for a spherical 6R closed chain there are more geometric parameters than the mechanism parameters and the effect of changing some geometric parameters has an unintended effect of influencing other parameters as well (e.g., changing location of the manifold also changes the size of the constraint manifold). Thus the functionality for changing geometric parameters has been disabled. The designer can still visually manipulate the constraint manifold using mechanism parameters.

4.2 Design Procedure for Spherical 6R Closed Chain

1. Use the Motion Design panel to input given positions, associated time parameter and interpolate them using a NURBS motion.

   The given spherical displacements can be input with the time parameter t, either using quaternion coordinates (q_1, q_2, q_3, q_4), or the latitude, longitude, and roll angles directly (θ, ϕ, ψ). Once all given positions are input, a cubic C^2 B-Spline motion that interpolates the given positions is generated. Consequently, the ISW shows the image points of the prescribed positions and renders a continuous NURBS curve which passes

through all the image points; while the CSW shows the given positions and the rational motion.

2. Switch to the Mechanism Design panel. Dimensional synthesis starts with two default 3R open chains. The procedure for one open chain is discussed below:

   In the CSW, the mechanism parameters are initialized to zero. As soon as the parameters are changed, in the ISW, a pair of hyperboloids appear. At this point, it will be apparent that the image curve is not completely contained between the inner and outer surfaces, which means that the constraints are being violated.

3. Modify the constraint manifold visually using the spinner controls (up and down arrows next to parameters) provided in the MeDP until the curve seems completely contained between the two pairs of hyperboloids. Dragging the slider in either ISW or CSW verifies if the constraints are actually satisfied or not. Using the current value of the mechanism parameters, the program automatically checks the constraint equations if they are satisfied. When they are satisfied, the program outputs links length and fixed and moving pivot locations.

4. Repeat steps 2, 3 and 4, and synthesize the other open chain.

4.3 Design Procedure for Planar Parallel Manipulator

1. Use the Motion Design panel to input given positions, associated time parameter, and interpolate them using a NURBS motion.

   The given planar positions can be input with the time parameter t, either using planar quaternion coordinates (Z_1, Z_2, Z_3, Z_4), or Cartesian coordinate directly (x, y, θ). Once all given positions are input, a cubic C^2 B-Spline motion that interpolates the given positions is generated. Consequently, the ISW shows the image points of the prescribed positions, and renders a continuous NURBS curve which passes through all the image points; while the CSW shows the given positions and the rational motion.

2. Switch to the Mechanism Design panel. Dimensional synthesis starts with the choice of RRR and RPR open chains. The procedure for RRR and RPR is the same hence only one open chain is discussed below:

   In the CSW, initially, the fixed pivots are located at $(x_1, y_1) = (0, 0)$; the three links have unit length $a_1 = b_1 = h_1 = 1$, and the relative angle of $\mathbf{M}$ to the floating link is $\alpha_1 = 0$. In the ISW, a pair of concentric and cooriented hyperboloids appear. The default hyperboloid pair is centered at $(0.5, 0, 0)$ and the inner boundary circle is of radius $r = L_{\min}/2 = 0$, while the outer one has a radius $r = L_{\max}/2 = 1$. At this point, it will be apparent that the image curve is not completely contained between

the inner and outer surfaces, which means that the constraints are being violated.

3. Modify the constraint manifold visually using the spinner controls (up and down arrows next to parameters) provided in the MeDP until the curve seems completely contained between the two pairs of hyperboloids. Dragging the slider in either ISW or CSW verifies if the constraints are actually satisfied or not. Using the current value of the mechanism parameters, the program automatically checks the constraint equations if they are satisfied. When they are satisfied, the program outputs links' length, fixed and moving pivot locations, and the orientation of the moving frame.

4. Repeat steps 2, 3 and 4, and synthesize the other two open chain.

5. Also note there can be several combinations to have a three legged planar parallel manipulator shown in the table[4.1].

4.4 An Example for Spherical 6R Closed Chain

In this section, an example is shown that demonstrates the dimensional synthesis of a spherical 6R closed chain using the constraint manifold modification for a given degree six B-spline rational motion.

In this example, we use five positions as given in Table 4.2, and shown in Fig. 4.2. The positions are given using quaternion coordinates, which specify the displacement of the moving frame **M**. Also given are the time parameter

ChainA	*ChainB*	*ChainC*
RRR	RRR	RRR
RRR	RPR	RRR
RRR	RRR	RPR
RPR	RRR	RRR
RPR	RPR	RPR
RPR	RRR	RPR
RPR	RPR	RRR
RRR	RPR	RPR

Table 4.1: Combinations of three legged planar parallel manipulator possible with the present software

i	q_1	q_2	q_3	q_4	u_i
0	0.1661	0.3322	0.4152	0.8305	0.0
1	0.0775	0.0930	0.6201	0.7751	0.2
2	0.0778	0	0.6228	0.7785	0.4
3	0.0685	0	-0.1957	0.9786	0.7
4	0	0	-0.7071	0.7071	1.0

Table 4.2: Quaternions of five prescribed positions along with their time parameter values

values (u_i) associated with each position. We note that we give the time parameter values to generate a B-spline image curve; as such they are not required for the rigid body guidance problems. The given positions are interpolated using a degree six NURBS motion. The corresponding image curve is shown in the image space window of Fig 4.2. The image curve is visualized using Rodrigues parameters (see Bottema and Roth [47]) given by $(Y_1/Y_4, Y_2/Y_4, Y_3/Y_4)$. Hereafter, two 3R open chains called A and B, and their constraint manifolds are initialized. However, navigating through the motion, it is found that the con-

straints are violated – this shows up as the image curve being outside the manifold. The designer next modifies the constraint manifolds by varying various parameters interactively until the curve is contained. Once the synthesis of two individual open chains A and B is completed, the assembly of A and B yields a 6R closed chain that passes through the given five positions with a continuous motion. Table 4.3 and 4.4 list the mechanism and the constraint manifold parameters, respectively.

	$\gamma(^\circ)$	$\alpha(^\circ)$	$\beta(^\circ)$	$\eta(^\circ)$
Open Chain A	30.12	12.60	58.65	43.40
Open Chain B	45.50	14.89	49.84	40.10

Table 4.3: Synthesis parameters of the spherical 6R closed chain

	inner hyperboloid center; orientation	outer hyperboloid center; orientation
Open Chain A	(1.5843,0,0);(0,0.1774,1)	(0.9805,0,0);(0,0.1378,1)
Open Chain B	(0.6323,0,0);(0,-0.6323,1)	(0.4691,0,0);(0,-0.4691,1)

Table 4.4: Synthesis parameters of the constraint manifolds

4.5 An Example for Planar Parallel Manipulator

In this section, an example is shown that demonstrates the dimensional synthesis of a planar parallel manipulator (RRR, RPR and RRR) using the constraint manifold modification for a given degree six rational motion.

i	x,	y,	$\theta(^\circ)$	u_i
0	0.0448	0.1940	0	0.0
1	1.2067	1.5029	30	0.3
2	2.894	1.4852	15	0.6
3	2.045	2.8478	9	1.0

Table 4.5: Cartesian coordinates of four prescribed positions along with their time parameter values

In this example, we use four positions as given in Table 4.5, and shown in Fig. 4.4. The positions are given in Cartesian coordinate (x, y, θ), which specify the location of origin of moving frame **M** and the relative angle of **M** to horizontal axis of the fixed frame. Also given are the time parameter values (u_i) associated with each position. First, the given positions are converted to planar quaternion representation (Z_1, Z_2, Z_3, Z_4) and then they are interpolated using a degree six NURBS motion. The corresponding image curve is shown in the image space window of Fig 4.4. The image curve is visualized using Rodrigues parameters (see Bottema and Roth [47]) given by $(Z_1/Z_4, Z_2/Z_4, Z_3/Z_4)$. Hereafter, one RRR open chains called A, one RPR open chain called B and another RRR open chain called C and their constraint manifolds are initialized. However, navigating through the motion, it is found that the constraints are violated – this shows up as the image curve being outside the manifold. The designer next modifies the constraint manifolds by varying various geometric parameters interactively. Different parameters have different effect on the size, position, and orientation of the manifold and the process is intuitive. Once the synthesis of three individual open chains A,B

and C is completed (see Figures. 4.5, 4.6 and 4.7), the assembly of A, B and C yields a planar parallel manipulator (see Fig. 4.3) that passes through the given four positions with a continuous motion. Table 4.6 lists the design results.

	x_1	y_1	a_1	b_1	h_1	α_1
Open Chain A (RRR)	3.0	0.0	4.2	3.8	4.0	0.0
	x_2	y_2	b_1	b_2	h_2	α_2
Open Chain B (RPR)	-1.5	-0.5	3.2	2.8	0.7071	2.3562
	x_3	y_3	a_3	b_3	h_3	α_3
Open Chain C(RRR)	-1.5	4.0	4.3	3.7	2.0616	-1.8158

Table 4.6: Synthesis parameters planar parallel manipulator

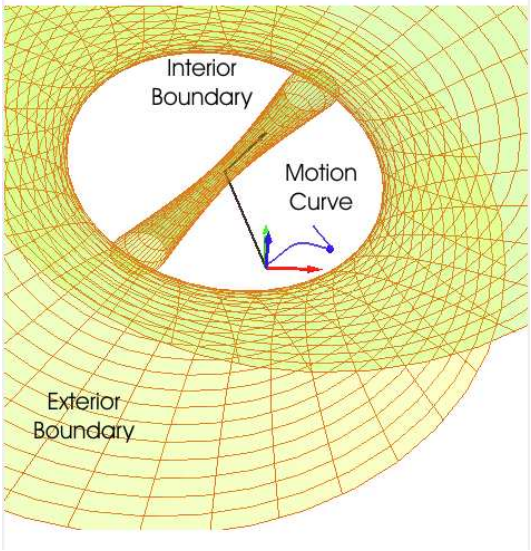

Figure 4.5: Constraint manifold of the RRR Open Chain A and image curve; in this figure, the image curve is completely contained inside the manifold, thus implying that the constraints are not violated.

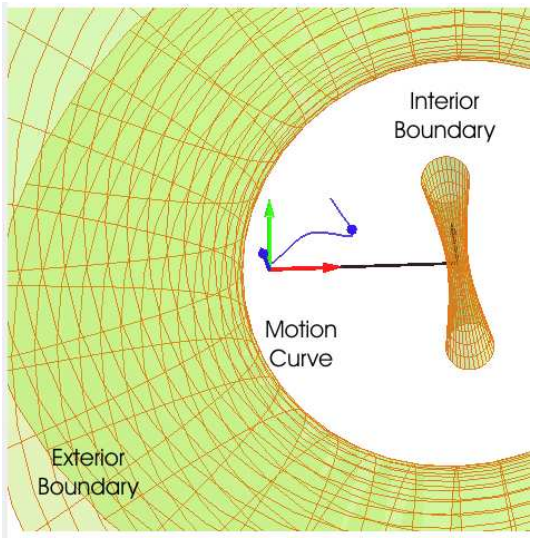

Figure 4.6: Constraint manifold of the RPR Open Chain B and image curve; in this figure, the image curve is completely contained inside the manifold, thus implying that the constraints are not violated.

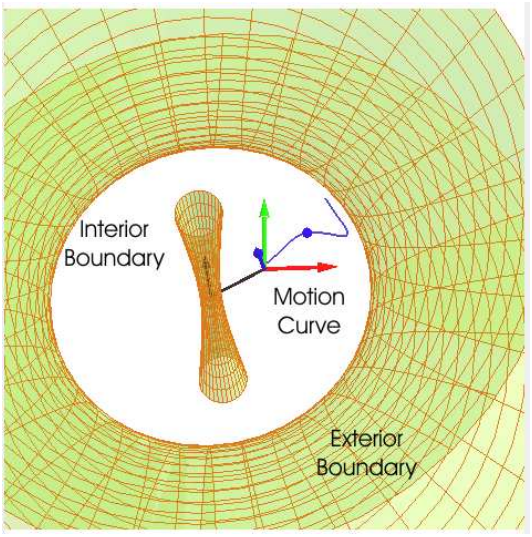

Figure 4.7: Constraint manifold of the RRR Open Chain C and image curve; in this figure, the image curve is completely contained inside the manifold, thus implying that the constraints are not violated.

Chapter 5

Conclusion and Future Work

Both 6R spherical closed chain and planar parallel manipulator have been successfully studied and implemented. The kinematic constraints of the spherical 6R closed chain and planar parallel manipulator have been discussed. Section[4] shows the implementation of both types of mechanism. The future work lies in both the spherical 6R chain as well as the planar parallel manipulator.

1. In the case of spherical 6R closed chain a search for a new hyperplane should be conducted so as to find a simple equation which has clear relations of the geometric and mechanism parameters. Presently, the hyperplane $Z_4 = 1$ is selected. If we change some geometric parameter it has an effect on changing some other parameters too(eg. change in location of manifold also changes the size of the constraint manifold).

2. The other case of planar parallel manipulator, the user has an option of two open chains RRR and RPR for the design of a planar parallel manipulator. That leads to eight different combinations of planar parallel

manipulator. The existing software can be extended to accommodate the other five(RRP, PRR, RPP, PPR and PRP) types of open chain.

To aid for extending the software a detailed documentation explaining all the classes, functions and variables extending to more than 30 pages has been prepared.

I see my work as an extension to the 6R planar closed chain software. There is a lot of scope for the expansion of this software containing all the other types of planar mechanisms.

It is hoped that this software aids researchers, students, professors as well as other professionals working in CAGD, Computational Kinematics, Motion Design and other related field.

Bibliography

[1] Sandor, G. N., and Erdman, A. G., 1997. *Advanced Mechanism Design: Analysis and Synthesis Vol. 2.* Prentice-Hall, Englewood Cliffs, NJ.

[2] Suh, C. H., and Radcliffe, C. W., 1978. *Kinematics and Mechanism Design.* Wiley, New York.

[3] McCarthy, J. M., 2000. *Geometric Design of Linkages.* Springer-Verlag, New York.

[4] RUBEL, A. J., and KAUFMAN, R. E., 1977. "Kinsyn iii: A new human-engineered system for interactive computer-aided design of planar linkages". *ASME Journal of Engineering for Industry,* **99**, p. 440448.

[5] Erdman, A., and Gustafson, J., 1977. Lincages: Linkage interactive computer analysis and graphically enhanced synthesis packages,. Tech. rep.

[6] Erdman, A. G., and Riley, D., 1981. "Computer-aided linkage design using the lincages package". In ASME Design Engineering Technical Conferences, ASME Press. Paper Number 81-DET-121.

[7] Kihonge, J., Vance, J., and Larochelle, P., 2001. "Spatial mechanism design in virtual reality with networking". In ASME 2001 Design Engineering Technical Conferences.

[8] Larochelle, P. M., 1998. "Spades: Software for synthesizing spatial 4c linkages". In ASME Design Engineering Technical Conferences (DETC).

[9] Perez, A., and McCarthy, J., 2000. "Dimensional synthesis of spatial rr robots". In Advances in Robot Kinematics.

[10] Su, H., and McCarthy, J. M., 2001. "Classification of designs for rrss linkages". In ASME Design Engineering Technical Conferences.

[11] Su, H., Collins, C., and McCarthy, J. M., 2002. "An extensible java applet for spatial linkage synthesis". In 2002 ASME Design Engineering Technical Conferences, ASME.

[12] SyMech. http://www.symech.com/.

[13] WATT. http://www.heron-technologies.com.

[14] Larochelle, P. M., Dooley, A. P., Murray, A. P., and McCarthy, J. M., 1993. "Sphinx: Software for synthesizing spherical 4r mechanisms". In NSF Design and Manufacturing Systems Conference, p. 607611.

[15] Ruth, D., and McCarthy, J. M., 1997. "Sphinxpc: An implementation of four position synthesis for planar and spherical 4r linkages". In ASME Design Engineering Technical Conferences (DETC).

[16] Furlong, T. J., Vance, J. M., and Larochelle, P. M., 1998. "Spherical mechanism synthesis in virtual reality". In ASME Design Engineering Technical Conferences (DETC).

[17] Tse, D., and Larochelle, P. M., 1999. "Osiris: a new generation spherical and spatial mechanism cad program". In 1999 Florida Conference on Recent Advancements in Robotics.

[18] Ketchel, J. S., and Larochelle, P. M., 2007. "Computer-aided manufacturing of spherical mechanisms". *Mechanism and Machine Theory,* **42**, p. 131146.

[19] Kraal, J. C., and Vance, J. M., 2001. "Vemecs: a virtual reality interface for spherical mechanism design". *Journal of Engineeing Design,* **12**(3), p. 245254.

[20] Chiang, C. H., 2000. *Kinematics of spherical mechanisms.* Krieger Pub., Malabar, FL. 00039067 C.H. Chiang. ill. ; 23 cm. Includes bibliographical references and index.

[21] Merlet, J. P., 2006. *Parallel Robots.* Springer.

[22] Ravani, B., and Roth, B., 1984. "Mappings of spatial kinematics". *Journal of Mechanisms Transmissions and Automation in Design-Transactions of the ASME,* **106**(3), pp. 341–347.

[23] Bodduluri, R. M. C., and McCarthy, J. M., 1992. "Finite position synthesis using image curve of a spherical four-bar motion". *ASME J. of Mechanical Design,* **114**(1).

[24] Bodduluri, R., 1990. "Design and planned movement of multi-degree of freedom spatial mechanisms". Ph.d. dissertation.

[25] Larochelle, P., 1994. "Design of cooperating robots and spatial mechanisms". Phd dissertation.

[26] Brunnthaler, K., Schrocker, H., and Husty, M., 2006. *Synthesis of spherical four-bar mechanisms using spherical kinematic mapping.* Advances in Robot Kinematics. Springer, Netherlands.

[27] Venkataramanujam, V., and Larochelle, P., 2007. "Approximate motion synthesis of spherical kinematic chains". In Proceedings of ASME 2007 International Design Engineering Technical Conferences & Computers and Information in Engineering, Paper No. DETC2007-34372.

[28] Larochelle, P. ., 2003. "Approximate motion synthesis of open and closed chains via parametric constraint manifold fitting: Preliminary results". In Proceedings of the 2003 ASME International Design Engineering Technical Conferences, ASME Press.

[29] Jin, Z., and Ge, Q. J., 2007. "Computer aided synthesis of piecewise rational motion for planar 2r and 3r robot arms". *ASME Journal of Mechanical Design,* **129**(10), pp. 1031–1036.

[30] Jin, Z., and Ge, Q. J., 2007. "Rational motion interpolation under kinematic constraints of planar 6r closed chain". In ASME 2007 International Design Engineering Technical Conferences & Computers and Information in Engineering Conference, ASME Press. Paper No. DETC2006-99650.

[31] Purwar, A., Zhe, J., and Ge, Q. J., 2008. "Computer aided synthesis of piecewise rational motions for spherical 2r and 3r robot arms". *ASME Journal of Mechanical Design,* **130**(11).

[32] Purwar, A., Jin, Z., and Ge, Q. J., 2008. "Rational motion interpolation under kinematic constraints of spherical 6r closed chains". *ASME Journal of Mechanical Design,* **130**(6), pp. 062301–1 – 062301–9.

[33] Purwar, A., Jin, Z., and Ge, Q. J., 2008. "Computer aided synthesis of rational motion under kinematic constraints of spatial ss open chains". In ASME 2008 International Design Engineering Technical Conferences & Computers and Information in Engineering Conference.

[34] Jun, W., Purwar, A., and Ge, Q. J., 2009. "Interactive dimensional synthesis and motion design of planar 6r single-loop closed chains via constraint manifold modification". In ASME 2009 International Design Engineering Technical Conferences and Computers and Information in Engineering Conference, ASME Press. Paper Number DETC2009-87818.

[35] McCarthy, J. M., 1990. *Introduction to Theoretical Kinematics.* MIT, Cambridge, Mass.

[36] Ge, Q. J., 1990. "Kinematics constraints as algebraic manifolds in the clifford algebra of projective three space". Ph.d. dissertation.

[37] Jin, Z., 2007. "Computer aided synthesis of rational motions under kinematic constraints". Ph.d. dissertation.

[38] Hayes, M. J. D., Zsombor-Murray, P. J., and Chen, C., 2004. "Kinematic analysis of general planar parallel manipulators". *ASME J. of Mechanical Design,* **126**(5).

[39] Merlet, J. P., 1996. "Direct kinematics of planar parallel manipulators". *IEEE Int. Conf. on Robotics and Automation.*

[40] Hayes, M., 1999. "Kinematics of general planar stewart-gough platforms". Ph.d. dissertation.

[41] Boehm, W., 1987. "Rational geometric splines". *Computer Aided Geometric Design,* **4**(1-2), pp. 67–77.

[42] Ravani, B., and Roth, B., 1983. "Motion synthesis using kinematic mappings". *Journal of Mechanisms Transmissions and Automation in Design-Transactions of the Asme,* **105**(3), pp. 460–467. Article.

[43] Larochelle, P., and McCarthy, J. M., 1994. "Design of spatial 4c mechanisms for rigid body guidance". In Proc. 1994 ASME Mechanisms Conference, pp. 135–142.

[44] Murray, A. P., Pierrot, F., Dauchez, P., and McCarthy, J. M., 1997. "A planar quaternion approach to the kinematic synthesis of a parallel manipulator". *Robotica,* **15**, pp. 361–365. Article Part 4.

[45] Perez, A., and McCarthy, J. M., 2004. "Dual quaternion synthesis of constrained robotic systems". *ASME Journal of Mechanical Design,* **126**(3), pp. 425–435.

[46] Hayes, M. J. D., and Husty, M., 2003. "On the kinematic constraint surfaces of general three-legged planar robot platforms". *Mechanism and Machine Theory,* **38**(379394).

[47] Bottema, O., and Roth, B., 1979. *Theoretical Kinematics*. North Holland, Amsterdam.